RSC Pharmaceutics

ROYAL SOCIETY OF CHEMISTRY

REVIEW

View Article Online
View Journal | View Issue

Cite this: *RSC Pharm.*, 2024, **1**, 879

A comprehensive investigation of the biophysical approach for aptamer functionalized nanoparticles in cancer therapy: a review

Alanthatta Govindan Navaneeth[a] and Subramani Karthikeyan *[b]

Received 25th October 2023,
Accepted 29th August 2024

DOI: 10.1039/d3pm00027c

rsc.li/RSCPharma

Aptamers stand out for their remarkable specificity and versatility, making them an invaluable tool in cancer therapy. When combined with nanoparticles, they form a dynamic platform for targeted drug delivery and diagnostics, leveraging enhanced cellular take up and the enhanced permeability and retention effect. This review explores both experimental and computational studies that probe the intricate interactions between aptamers and nanoparticles. By combining theoretical insights with empirical studies, this approach deepens our understanding of aptamer–nanoparticle conjugation, opening new avenues to enhance therapeutic efficacy and reduce off-target effects. Recent advancements in the field are critically analysed, spotlighting transformative studies that highlight the potential of this approach. Offering a comprehensive overview of current achievements and future prospects, this article aims to establish the pivotal role of aptamer-functionalized nanoparticles in personalized cancer treatment strategies.

[a]*Department of Physics, School of Advanced Sciences, Vellore Institute of Technology (VIT), Chennai Campus, Vandalur-Kelambakkam Road, Chennai - 600127, India*
[b]*Center for Health Care and Advanced Research, Vellore Institute of Technology (VIT), Chennai Campus, Vandalur-Kelambakkam Road, Chennai - 600127, India. E-mail: s.karthikeyan@vit.ac.in*

1. Introduction

Cancer is currently one of the most serious threats to public health, causing numerous fatalities every year. It results from

Alanthatta Govindan Navaneeth

A. G. Navaneeth is currently pursuing a Ph.D. in Physics at Vellore Institute of Technology University Chennai Campus, Chennai-127, with a research emphasis on nano-mediated targeted drug delivery, sensing, and imaging for cancer therapy. His academic journey commenced in 2016 with a Bachelor of Science degree in Physics from Kannur University, where he laid the groundwork for his interest in scientific inquiry and exploration. Subsequently, he earned his Master's degree in Physics at SDM College, Mangalore University (2017–2019). Presently, he is dedicated to his Ph.D at VIT Chennai, focusing on harnessing nanotechnology to develop innovative approaches for targeted drug delivery, sensing, and imaging in cancer treatment. His work aims to enhance the precision and effectiveness of cancer therapy while minimizing the adverse effects associated with conventional treatments.

Subramani Karthikeyan

Dr S. Karthikeyan is currently working as an assistant professor at the Centre for Healthcare Advancement Innovation and Research (CHAIR), Vellore Institute of Technology University Chennai Campus, Chennai-127. He obtained his Master's in Biophysics from the Centre of Advanced Studies in Crystallography and Biophysics, University of Madras (2011–2013), and his Ph.D. from the Department of Medical Physics, Guindy Campus, Anna University (2014–2018). He worked as a junior scientist at a research institute of organic chemistry, People's Friendship University of Russia (RUDN University), Moscow, Russia. His primary research interest is to understand the binding interaction mechanism between various heterocyclic molecules and respective target protein/DNA molecules using various biophysical techniques. He believes that such biophysical techniques will help to design and develop effective drugs in the field of bio-medicine in the near future.

multiple factors, including genetic, lifestyle, and environmental factors. According to GLOBCAN, from 2020 to 2040, the number of cancer cases in India will increase by 57.5%, reaching 2.08 million. China has the highest number of cancer cases worldwide; India ranks third, behind China and the United States.[1] Even though cancer is referred to as a single condition, it is a group of diseases characterised by the uncontrolled growth and spread of abnormal cells. These abnormal cells can invade and destroy neighbouring tissues, and they can also travel throughout the body *via* the bloodstream or lymphatic system.[2] When cancer progresses to a metastatic state or begins to spread to nearby organs, a systemic chemotherapy approach is required for effective cancer management. In chemotherapy, the chemodrugs circulate in the bloodstream and kill the rapidly growing cancer cells. Normal cells in hair follicles and bone marrow also rapidly develop, since chemodrugs attack all rapidly growing cells, they are unable to differentiate these normal healthy cells from cancerous cells, which leads to numerous side effects, such as anaemia, gastrointestinal problems, vomiting, and nausea.[3–5] In order to overcome this limitation, a distinct strategy with fewer off-target effects and high treatment efficacy is required. Targeted drug delivery is one of the possible solutions for meeting this need. In this particular treatment modality, a carrier will transport the drug molecule to the desired location, with nanomaterials serving as one such carrier. Nanomaterials are used to transport various types of molecules, such as nucleic acids, proteins, and microRNA.[6] The major feature that makes nanoparticles appropriate for cancer therapeutic applications is their size, which ranges from 5 to 100 nm. Furthermore, it improves biodistribution and dosage tolerance for cancer cells, improves the solubility of poorly soluble medicines and slows down their metabolism.[7] The physical phenomenon that promotes nanoparticle accumulation in tumour tissues is known as the EPR (enhanced permeability and retention) effect, which is illustrated in Fig. 1. The factor that facilitates the EPR effect is abnormal angiogenesis.[8] This is one of the defining characteristics of malignancy, characterized by the uncontrolled growth of blood vessels. Due to their rapid growth, these blood vessels are porous and irregular. The size of these pores can range from a few hundred nanometers to micrometers.[7] Nanoparticles with diameters between 10 nm and 100 nm are ideally sized to pass through the gaps in these blood vessels.[9]

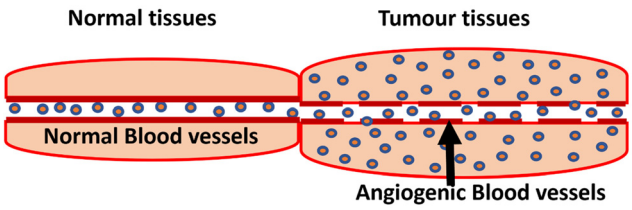

Fig. 1 EPR (enhanced permeability and retention) effect inside the circulatory system, in which nanoparticles penetrate tumour cells *via* angiogenic blood vessels but do not enter healthy cells due to the small pore size. The red tube-like structure represents the blood vessels, the red tube-like structure with large pores represents angiogenic blood vessels, and the red spheres represent the drug conjugated nanoparticle.

Active targeting increases the EPR effect by adding tumour-specific ligands to the surface of nanoparticles. To achieve this, a range of targeted ligands such as aptamers, antibodies, antibody fragments, human transferrin proteins, sugars, peptides, and vitamins such as folate, *etc*. are employed. The functionalized nanoparticles penetrate the tumour through the EPR effect, and then the targeting ligand binds to the cancer biomarker; this may increase the retention time of the nanocarrier–drug combination inside the tumour cell.[10] Aptamer conjugated nanomaterials may offer a safer and more efficient way to fulfil the growing demand for new cancer treatments by combining the features of nanomaterials with the unique identification capacity of aptamers.[11]

In our comprehensive review, we embark on a journey through the intricate biophysical mechanisms that underpin the functionalization of nanoparticles with aptamers, specifically tailored for cancer therapy. Delving deep into the art of aptamer selection, the nuances of aptamer–nanoparticle design, and the critical factors influencing their interactions, we aim to provide a panoramic understanding of this cutting-edge approach. We explore the latest experimental and computational techniques employed to characterize these functionalized nanoparticles, illuminating their potential to redefine targeted cancer treatment. By unravelling both the promising advancements and challenges in this dynamic field, our insights aim to chart a course towards future innovations in cancer therapy.

2. Aptamers: history and background

Tuerk introduced the term "aptamer", which is derived from the combination of the Latin word aptus ('to fit') and Greek word meros ('part'), in 1990 to describe short single- or double-stranded DNA or RNA molecules.[12] They are generated from a pool of random sequences, through a method known as SELEX. To date, thousands of aptamers have been selected against a wide range of targets, including metal ions, viruses, bacteria, peptides, proteins, cells, and even targets within live animals.[13,14] Aptamers show great affinity for their target with a K_d value in the nanomolar to picomolar range.[15] Also, the high selectivity of aptamers can differentiate closely related isoforms of the same target molecule. For example, theophylline, theobromine and caffeine have similar structures. Theobromine is an isomer of theophylline with a methyl group in a different position and caffeine differs from theophylline by a single methyl group. The anti-theophylline RNA aptamer shows high discrimination against both of these analogues, and it is proved that the binding affinity of the RNA aptamer with theophylline is 10 000 times higher than that with caffeine.[16] The aptamers are capable of maintaining their binding and inhibitory activity even after being immobilised

on carrier material, labelled with different functional groups, and expressed in living cells. Furthermore, their characteristics such as the ability to directly bind with targets, high resistance to various pH and organic solvent environments, low immunogenicity and cytotoxicity, strong chemical stability, molecular weight, and the potential to discover new signature molecules, make them promising candidates for different applications such as target validation, purification processes, drug discovery, therapy, and diagnostics.[17–20]

Nucleic acid aptamers, including DNA and RNA, exhibit similar properties but differ notably in chemical stability and target accessibility. RNA aptamers are chemically less stable due to the presence of a reactive hydroxyl group, whereas DNA aptamers, which lack this group, are more chemically stable. The functionality of both DNA and RNA aptamers relies on their stable three-dimensional structures, influenced by the primary nucleotide sequence, the length of the nucleic acid molecule, and environmental conditions. Typically, aptamers range in size from 25 to 100 nucleotides.[21] Common structural motifs include internal loops, stems, hairpin structures, purine-rich bulges, pseudoknots, tetra loops, and G-quadruplexes.[22] In 1993, Bock *et al.* reported the first protein-targeted DNA aptamer, a 15-nucleotide sequence against human thrombin.[23] This DNA aptamer features a stacked G-quartet structure, similar to natural single-stranded DNAs, and was developed to inhibit thrombin-catalyzed fibrin clot formation with a binding constant (K_d) of 200 nmol L^{-1}. Additionally, thrombin-specific RNA aptamers have been developed. In 1994, Kubik *et al.* introduced the first RNA aptamer that selectively bound to thrombin's heparin site, reporting a K_d value of 2–5 nmol L^{-1}, indicating a tenfold higher affinity compared to the DNA aptamer targeting the same protein.[24] This demonstrates that the RNA aptamer has a higher affinity for thrombin than its DNA counterpart. Subsequently, White *et al.* developed an RNA aptamer targeting the fibrinogen binding site of thrombin.[25] Later, Gronewold *et al.* investigated the binding affinity of this RNA aptamer using surface plasmon resonance, binding assays, and acoustic methods, reporting K_d values of 113 nmol L^{-1}, 294 nmol L^{-1}, and 181 nmol L^{-1}, respectively.[26]

Peptide aptamers, unlike nucleic acid aptamers, are artificial proteins engineered to bind specific target molecules. According to Colas *et al.*, a peptide aptamer is a combinatorial protein molecule with a variable peptide sequence that shows affinity for a target protein and is displayed on an inert scaffold protein.[27–29] Because both termini of the variable sequence are fused to the scaffold protein, peptide aptamers are doubly constrained.[28,30] This double constraint sets them apart from other artificial combinatorial proteins, which typically consist of a peptide sequence terminally fused to the target protein. Peptide aptamers exhibit molecular recognition similar to antibodies but with enhanced characteristics such as small size, high-yield bacterial expression, rapid folding properties, high solubility, high stability, and the possibility of chemical synthesis. Interestingly, the binding affinity of these combinatorial proteins is increased by the constraints imposed by the scaffold[31] (Fig. 2).

3. SELEX-aptamer generation

Craig Tuerk and Larry Gold first introduced the idea of SELEX (systematic evolution of ligands by exponential enrichment). They used this method to select an RNA sequence targeting T4 DNA polymerase from a combinatorial library of random sequences.[12] Theoretically, this library contains 4^N modified or unmodified single-stranded oligonucleotide sequences, created by standard organic synthesis. The SELEX process primarily involves three steps: (1) incubating a library of randomized sequences with a target molecule, (2) separating the bound sequences from the unbound ones, and (3) collecting and amplifying the bound sequences using PCR.[33] This selection process is repeated until the sequences with the desired affinity for the target are enriched. The basic methods for aptamer selection have remained largely the same; there have been significant advancements in several areas, including characterisation, target types and modification (how aptamers can be modified for different applications).[34]

Recent advancements in computerized analysis and sequencing technologies have enhanced our understanding of aptamer dynamics during the selection process. This progress will help identify effective sequences with high affinity in a shorter time.[35] Additionally, new polymerases have been introduced to create sequence libraries with high nuclease hydrolysis stability, reducing the need for labour-intensive post-selection modifications. To further enhance serum stability for therapeutic applications, various derivatives with modifications on the sugar rings are used to incorporate unnatural nucleotides into oligonucleotides.[36] These modifications include 2′-fluoro (2′-F) ribose, 2′-amino (2′-NH_2) ribose, 2′-*O*-methyl (2′-OMe) ribose, and locked nucleic acids (LNAs), which bridge the 2′ and 4′ positions of ribose covalently.[34]

4. Aptamer–target interactions in SELEX

The interaction between the aptamer and its target is the primary factor that determines the effectiveness and quality of the SELEX process.[37] The efficiency of this interaction is influenced by several variables, including the secondary structure of the aptamer, the diversity of aptamer sequences, the type and size of the target molecule, the immobilization matrix, physicochemical properties, and chemical modifications.[38,39] It is critical to characterise this aptamer–target interaction for the tailoring of an aptamer with good affinity. Several biophysical instruments or techniques have been developed to measure aptamer–target binding affinity, including capillary electrophoresis (CE), isothermal titration calorimetry (ITC), surface plasmon resonance (SPR), circular dichroism (CD), microscale thermophoresis (MST), photonic crystal surface waves (PC SWs), and a quantum crystal microbalance (QCM). CD and CE are used to investigate the aptamer's conformational changes upon binding to its target. Similarly, SPR, PCSW, and QCM are used to monitor the affinity interaction and

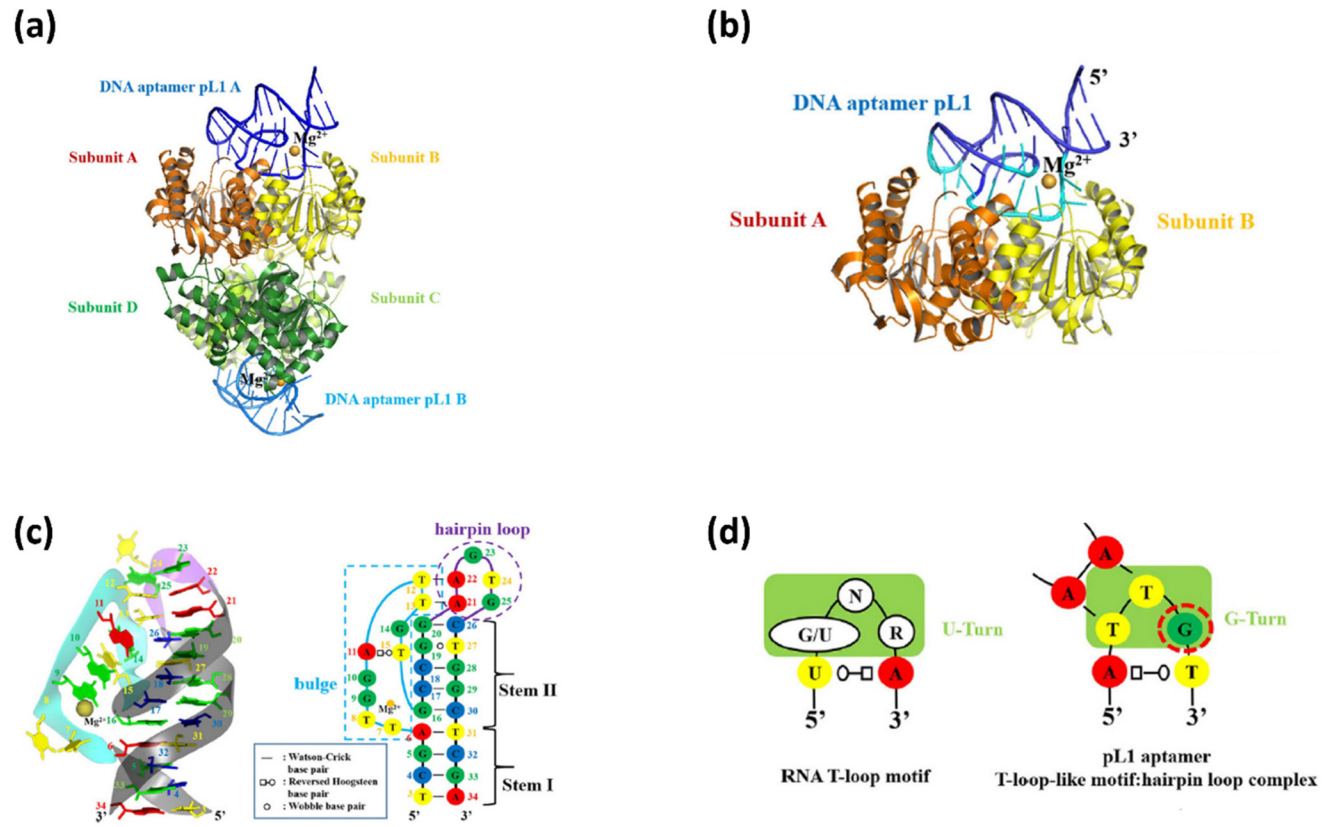

Fig. 2 Overall structures of PvLDH complexed with pL1 that fold into a hairpin–bulge contact, gold sphere represents a magnesium ion, (a) tetrameric PvLDH interacts with two DNA aptamers; PvLDH subunits A, B, C, and D are coloured orange, yellow, light green, and dark green, respectively. pL1 A and B are coloured blue and marine blue, respectively. (b) Dimeric PvLDH interacts with a DNA aptamer. PvLDH subunits A and B are coloured orange and yellow, respectively. (c) The structure and schematic of a DNA aptamer pL1. Ribbon depiction of pL1, with secondary structure. The strands comprising the bulge, hairpin loop, and stems are coloured cyan, purple, and black. (d) A comparison of RNA T-loop and DNA T-loop-like motifs that induce the hairpin–bulge interaction. N symbolises nucleotides, while R stands for purine. The nucleotides at the T and G turns are boxed in yellowish green. Adenine, guanine, thymine, and cytosine are coloured red, green, yellow, and blue, respectively.[32]

related kinetics in real time. ITC and MST are employed to investigate the thermodynamic properties of the aptamer–target interaction[38,39] (Fig. 3).

5. The factors influencing aptamer–target interactions

5.1 Target molecule

The interaction between an aptamer and its target is influenced by the structure, shape, and dimensions of the target molecule. The target molecule can be either smaller or larger than the aptamer. When the target molecule is smaller, such as aromatic ligands, ions, oligosaccharides, or charged amino acids, it integrates into the aptamer structure. This interaction is typically facilitated by stacking interactions (with flat aromatic ligands and ions),[38–40] electrostatic complementarity (with oligosaccharides and charged amino acids),[41,42] or hydrogen bonding.[43–46]

In contrast, if the target molecule is a larger protein, the aptamer integrates into the protein structure or attaches to its surface. Due to protein's complex structure, this interaction is more diverse.[42,47,48] However, hydrogen bonding still plays a significant role in this interactions.

5.2 Aptamer structure complexity and stability

The next factor influencing aptamer–target interactions is the structural complexity of the aptamer. Due to sequence-dependent propensities, aptamers can assume a multimeric state by forming G-quadruplexes or i-motifs, both of which facilitate interactions between multiple oligonucleotides.[41–43] According to the "induced fit" principle, the formation of an aptamer–target complex can result in conformational changes to the target, the aptamer, or both.[44–46] This induced fit leads to structural complementarity, influencing short-range interactions such as hydrogen bonding and van der Waals contacts. Conformational changes can also lead to catalytic activity, where the aptamers are known as aptazymes. The negative charges on the surface of the target can negatively impact the aptamer–target interactions due to repulsive interactions with the highly electronegative phosphate groups in DNA and RNA.[47,48] While positive charges can enhance the interaction

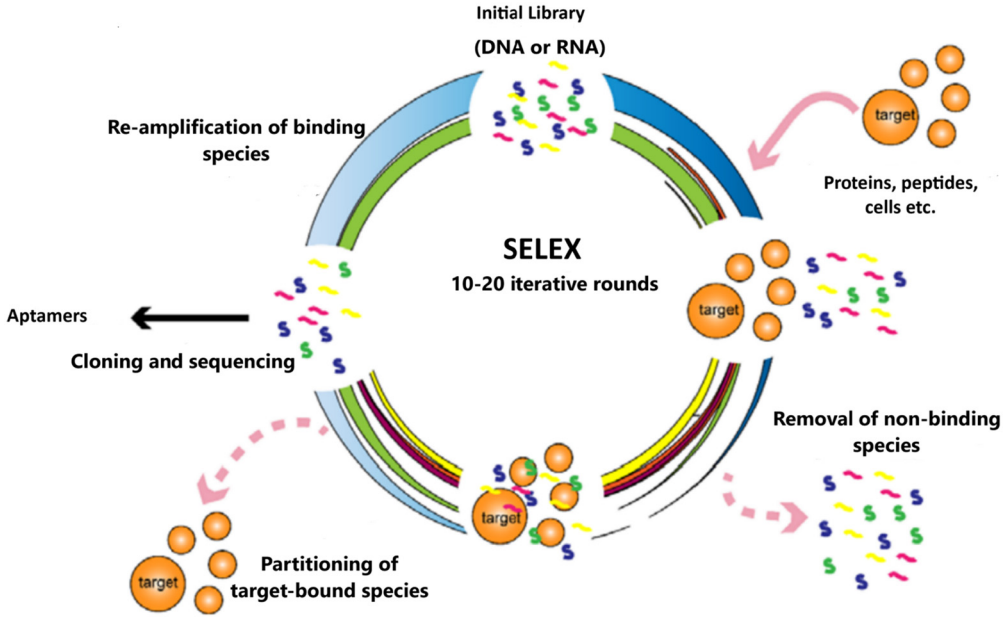

Fig. 3 Schematic illustration of the SELEX process for the DNA and RNA library.[40]

strength, they may also increase the likelihood of non-specific binding. Generally, aptamers are hydrophilic, making them less likely to interact with hydrophobic targets.[49,50]

In biological systems, the stability and functionality of unmodified aptamers are compromised by nuclease degradation.[51,52] The stability of aptamers in intracellular environments, which is a major concern for therapeutic applications, can be enhanced from minutes to hours through chemical modifications or by selecting polyvalent aptamers.[53] Additionally, pre-SELEX and post-SELEX chemical modifications play a crucial role in tailoring aptamers for various applications. This enhancement can be achieved through terminal modifications, such as adding modified nucleotides to the aptamer backbone, or by nucleotide modifications using different nucleic acids.[54]

In 2012, Li *et al.* introduced a polyvalent aptamer with multivalent interactions for increasing the nuclease stability. This is accomplished by covalently linking desired linkers to aptamers or by combining nanoparticles with aptamers.[55] In addition, the polyvalent aptamers have a low dissociation constant, and thus, a higher binding affinity. Seferos *et al.* developed a gold nanoparticle–polyvalent oligonucleotide complex with enhanced nuclease stability.[56] This complex features, a 13 nm gold nanoparticle (Au NP) functionalized with both antisense oligonucleotides and synthetic peptides. It exhibits perinuclear localization and enhanced gene regulation activity when tested in cellular models.

5.3 pH and temperature

The tertiary complex formed between an aptamer and its target is stabilized through a binding mechanism that relies on protonation.[57] If the pH is greater than the critical pK_a value of the target, the aptamer–target complex may form *via* hydrogen bonding. However, when the pH is lower than the pK_a of the target, binding-linked protonation prevents the target from binding to the aptamer. Plich *et al.* found that the pH of an RNA–aminoglycoside complex affected its thermodynamic stability. They also observed that the protonation at acidic pH decreased aptamer–target coulombic repulsion, leading to prolonged retention times.[58] The interaction between the aptamer and its target molecule involves thermodynamic processes such as entropy and enthalpy.[59] Therefore, temperature significantly influences binding affinity. According to McKeague *et al.*, the optimal temperature for achieving optimal binding kinetics and high affinity is approximately 37 °C.[60]

6. Types of SELEX

6.1 Capillary electrophoresis SELEX

Capillary electrophoresis (CE) serves not only as a selection tool but also as an analytical technique capable of determining binding affinity and monitoring the enrichment of ssDNA in each round of selection cycles, as well as assessing the quality of both the target and the ssDNA library. It offers advantages over other conventional SELEX methods, such as enhanced analysis capabilities, reduced sample and analytical reagent consumption, and improved screening efficiency.[61–65] CE-SELEX typically requires only 1–4 rounds for aptamer selection, significantly reducing selection cycles and time.[66,67] Furthermore, in CE-SELEX, aptamer binding and separation take place in free solution, eliminating steric hindrance of the interaction. Although all conventional SELEX methods, including CE-SELEX, rapid-SELEX, and microfluidic SELEX, necessi-

tate prior knowledge of the target, they also require purified protein for aptamer selection. Consequently, aptamers selected *in vitro* using these methods often fail to recognize their target proteins in their native conformation. Traditionally, CE-SELEX was primarily associated with selecting aptamers for large protein targets. However, in recent times, this technique has been successfully employed to select aptamers that target small peptide molecules such as neuropeptide Y, which has a size of 4272 Da—smaller even than DNA. With small molecule targets, the mobility of the complex changes minimally compared to non-binding sequences, posing challenges in distinguishing between binding and non-binding sequences. Nonetheless, PCR can exponentially amplify nucleic acids even from small sample amounts, enabling sufficient enrichment. Bowser's team pioneered the concept of CE-SELEX, applying it to proteins, peptides, and small molecules.[65,68] They utilized high-throughput sequencing techniques to analyze the evolution of sequence enrichment and affinity differences. Using this approach, Bowser and Mendonsa successfully selected an aptamer targeting IgE (with a K_d of less than 30 nM) after just four rounds of selection.[68] These efforts represent significant advancements and innovations in SELEX. In 2005, Mosing *et al.* also employed this method to develop an aptamer for HIV reverse transcriptase following four rounds of selection.[69]

6.2 Toggle SELEX

Many potential therapeutic molecules show excellent *in vitro* activity but often fail to progress to clinical trials due to their lack of expected efficacy *in vivo*. This discrepancy may stem from molecules developed to target human proteins exhibiting lower affinity for analogous proteins in animal models.[25] To address this issue, innovative models enable the substitution or insertion of human homologues into other species. For example, the *in vivo* efficacy of a human L-selectin aptamer was demonstrated in a xenogeneic model (SCID mouse/human lymphocyte),[70] although such approaches are costly and less feasible. In response to these challenges, White *et al.* introduced a novel selection technique aimed at enhancing the development of therapeutic molecules that exhibit cross-reactivity between species.[25] They introduced the concept of toggle SELEX to develop aptamers that were clinically relevant in humans and testable in animal models. Using this cross-reactive selection strategy, they successfully created a nuclease-resistant RNA ligand capable of binding to both human and porcine thrombin by alternating the protein target between these two species during selection rounds. Such aptamers demonstrate the ability to inhibit both porcine and human thrombin activity.[25]

6.3 Microfluidic SELEX

Serum comprises a diverse array of components, including proteins, enzymes, lipids, hormones, small molecules, and electrolytes. In this technique, aptamers are selected against a serum pool. Initially, the nucleotide library undergoes negative SELEX to eliminate sequences binding to normal serum components, thereby enhancing the affinity of the isolated aptamers.[71] This refinement step improves the effectiveness of the selection process,[72] enabling the creation of highly specific and selective aptamers suitable for various applications. Using this approach, aptamer apt-5 was isolated, which targeted human CLEC3b and demonstrated significant impacts on tumour immunity and infection.[73,74] Additionally, Li *et al.* identified six distinct aptamers by utilizing serum samples from individuals with lung cancer.

6.4 Cell-SELEX

The *in vitro* method used for selecting aptamers against living cells is known as cell-SELEX.[75] This approach is effective at identifying high-affinity aptamers against various targets, such as the purified extracellular domain of prostate-specific membrane antigen (PSMA),[76] pure MUC1 peptides,[77] protein tyrosine phosphatase 1B (PTP1B),[78] and the cell adhesion molecule P-selectin.[79] The initial application of cell-SELEX involved targeting the pathogenic organism *Trypanosoma brucei*.[80] The study led to the discovery of three RNA aptamers that specifically targeted the effective bloodstream life cycle stage of the parasite. These aptamers are directed towards the parasite's flagellar pocket; however, none of them exhibit binding to VSG proteins, which are highly prevalent polypeptides on the trypanosome's surface.

The cell-SELEX technique, predominantly utilized in cancer therapy, generates a range of aptamers aimed at different types of cancer cells. These encompass cells originating from human hepatocarcinoma, mouse tumour endothelial cells, small cell lung cancer, glioblastoma multiforme, lung adenocarcinoma, colorectal cancer, and prostate cancer. Compared to conventional SELEX, cell-SELEX offers numerous advantages. For instance, this technology enables the identification of both established and novel biomarkers present on the cell membrane surface.[81] Cell-SELEX specifically targets live cells with a multitude of surface molecules, facilitating the development of a diverse panel of aptamers. This capability is invaluable for precise disease diagnosis. Daniel *et al.* isolated a pool of highly specific DNA aptamers by targeting the glioblastoma-derived cell line U251. They subsequently identified and characterized tenascin-C as a target protein for one of the isolated oligonucleotides; this is an extracellular protein found in the tumour matrix.[82] However, the selected aptamer exhibits reduced affinity at physiological pH and is susceptible to nuclease degradation. Subsequently, Hicke *et al.* described a modified DNA aptamer stabilized against nucleases, targeting tenascin-C. This aptamer binds specifically to the fibrinogen-like domain of tenascin-C.[75] While this technique offers significant benefits, it also presents certain technical challenges. Specifically, selecting an aptamer against a target protein that is expressed at low levels on the cell membrane can be difficult. In cell-SELEX, it is critical to avoid erroneous binding caused by cell death and dying cells during the selection process, as this can diminish the overall quality of the selection.[84] Therefore, high-speed fluorescence-activated sorting

Table 1 Illustration of several cell-SELEX selected aptamers, their targets, and the types of cancer for which they are useful

Aptamer	Target	Cancer type	Ref.
TTA1	Matrix protein, tenascin-C	Breast, glioblastoma, lung and colon cancer	Hicke *et al.*[77]
AS1411	Nucleolin (plasma membrane of cancer cell)	Breast, prostate, lung, pancreatic cancer and renal carcinoma	Girvan *et al.*[78]
MUC-1	Mucin (expressed on human adenocarcinomas)	Lung cancer	Ferreria *et al.*[79]
Apta-3, Apta-5	Carcinoembryonic antigen (CEA) in T84 cells	Colorectal cancer	Melo *et al.*[80]
Apc1	Caco2		Li *et al.*[81]
SKBR-3-R_1 Tr	Luminal A breast cancer subtype $SKBR_3$ cells	Breast cancer	Ferreira *et al.*[82]
Ag-9, Ag-9g, A_{10}, $A_{10\text{-}3}$, A_{10} L, $A_{10\text{-}3.2}$, $A_{10\text{-}3\text{-}J}$	PSMA	Prostate cancer	Lupold,[83] Leach *et al.*,[84] Dassie *et al.*,[85] Rockey *et al.*[86]
HPV-07	Type-16 virus-like-particle	Cervical cancer	Rockey *et al.*,[86] Trausch *et al.*[87]
c-9s	Ca ski cells, HeLa cells		Wang *et al.*[71]
Seq-3, seq-6, seq-19 and seq-54	Circulating tumour cells	Gastric cancer	Li *et al.*[88]
Spl3 EN-2 binding	Cyto-skeleton associated protein-4	Bladder cancer	Kim *et al.*[89]
ssDNA aptamer	Engrailed 2 (EN-2)		Sun *et al.*[90]

(FACS) can be employed to effectively separate live cells from dead ones.[76]

To date numerous aptamers have been developed by using cell-SELEX to diagnose different types of cancers, which includes glioblastoma, leukaemia, cholangiocarcinoma, liver cancer and breast cancer; these aptamers have also been applied in cancer classification and treatment. Zhao *et al.* explored the specificity of four aptamers (s1, s6, s11e, and s15) selected for adenocarcinoma A549, evaluating them across different cancer cell types.[73] Their study revealed that while all four aptamers could detect adenocarcinoma cells, only s11e could identify both types of squamous carcinoma cells. This research highlights the potential of these aptamers in differentiating between distinct subtypes of large carcinoma cells. Moreover, the binding affinities of these four aptamers to different samples of large carcinoma cells vary, suggesting their capability to discern molecular distinctions. In a related study, Shangguan *et al.* isolated a DNA aptamer, sgc8c, specifically targeting the T cell acute lymphoblastic leukemia cell line CCRF-CEM, with a focus on diagnosing acute lymphoblastic leukemia.[100] They demonstrated that sgc8c could detect leukemia cell lines in human bone marrow samples obtained from clinical specimens, highlighting its promise as a molecular probe for cancer detection. Suwussa *et al.* developed ACMNPs (aptamer-conjugated magnetic nanoparticles) capable of distinguishing between various types of cancer cells.[91] This study involved selecting different aptamers—sgc8c targeting CCRF-CEM cells, KDED2a-3 targeting DLD-1 cells, and KCHA10 targeting HCT 116 cells—and coupling them with magnetic nanoparticles. These nanostructures exhibit enhanced stability and are employed for cancer detection. The specificity and selectivity of the aptamer–nanoparticle complexes were evaluated in diverse complex biological environments and cell mixtures, including fetal bovine serum albumin (BSA), whole blood, and human plasma. Notably, in a 1 : 100 mixture of target and non-target cells, the sgc8c aptamer–NP complex demonstrated high sensitivity. Similarly, the selectivity of the other two aptamer complexes was also found to be high. For further details, refer to Table 1, which lists the variety of aptamers selected through cell-SELEX, their targets, and the corresponding cancer types.

6.5 Tissue SELEX

Generally, for isolating aptamers against live cells, cell-SELEX is developed as a modified SELEX strategy that uses the living cell as the target. However, this process is time consuming and laborious, and the binding affinity and specificity of the selected aptamers are highly dependent on the selection process.[92] In addition, the primary cultured cell line cannot reflect the actual *in vivo* tumour occurrence and development, which limits the clinical application of the cell-SELEX aptamers. Accordingly, a new variant of the selection technique known as tissue SELEX is introduced. Tissue SELEX enables the identification of aptamers against different target molecules, including membrane components and intracellular substances. As an example, Li *et al.* developed aptamer BC15 by targeting the intracellular protein hnRNP A1 through tissue-based SELEX.[92] By using tissue SELEX, Zhong *et al.* isolated aptamer TC-16, which showed high affinity and specificity for papillary thyroid carcinoma (PTC).[93]

6.6 Bead based SELEX

Immobilizing target molecules on various solid supports, such as agarose, Sepharose, and Sephadex, is a commonly used approach in SELEX.[94] Bead-based SELEX can be performed in two ways: first, by immobilizing the target on a solid support and then incubating it with an oligonucleotide library; second, by incubating the target with an oligonucleotide library and then selecting the best aptamer–target complex based on the highest affinity interaction.[95,96] In both methods, steady-state equilibrium binding occurs, while non-equilibrium binding under flow conditions occurs only in the first method. This

enables users to select aptamers based on various kinetic parameters. In the pre-immobilization scenario, the density of the target molecule on the solid support is crucial, as it influences the enrichment of aptamer sequences in each round of SELEX. An example of bead-based selection is the isolation of a DNA aptamer against staphylococcal enterotoxin B (SEB).[97] Another example is the isolation of a PDL-1 (programmed death ligand 1) specific aptamer with a K_d value of 64.77 nM after 10 rounds of SELEX to serve as a cancer biomarker.[28]

6.7 SPR-SELEX

The primary reason that conventional SELEX is time-consuming is that selecting and evaluating the binding affinity of an aptamer is a two-step process.[94] SPR-SELEX addresses this limitation by evaluating pool enrichment in real-time, round by round, during the selection process. This method monitors binding by tracking the SPR signal during pool injection and partitioning. If no further evolution occurs in the SPR signal, the selection procedure can be stopped. SPR-SELEX accelerates aptamer isolation by simultaneously selecting and evaluating binding sites. This approach is applicable to any type of target, provided that the oligonucleotide–target dissociation does not exceed the instrument's recovery time. Dausse *et al.* successfully employed SPR-SELEX to isolate a high-affinity RNA aptamer (K_d value = 8 nM) that formed stable loop–loop complexes with the target after six rounds of selection.[98]

7. Aptamer-conjugated nanoparticles in targeted drug delivery

Aptamers serve as ideal targeting ligands for functionalizing nanomaterials in various applications such as therapies, diagnostics, and drug delivery. Despite showing promising results in preclinical tests, aptamer–nanoparticle complexes have not yet progressed to the clinical stage of therapeutic development.[11] Table 2 details the aptamers utilized to functionalize nanoparticles for targeted cancer therapy, emphasizing their potential to enhance the precision and effectiveness of cancer treatments.

8. Aptamer–nanoparticle conjugation

The direct or indirect attachment of an aptamer to a nanoparticle is achieved using a linker molecule, often referred to as a spacer or bridge. Additionally, this conjugation can occur through covalent or non-covalent interactions.[11] Typically, covalent conjugation occurs when functional groups at the end of an aptamer interact with functional groups on the nanoparticle's surface. Common functional groups on an aptamer include primary amino groups and thiol groups, while nanoparticles may have carboxylic acid groups, aldehyde groups, or maleimide groups on their surfaces.[10,122,123] Moreover, the interaction of aptamer functional groups with linker molecules, metal ions, and inorganic molecules in nanoparticles also facilitates covalent conjugation. Common types of covalent bonds in aptamer–nanoparticle conjugation include amide linkages, thioester bonds formed from the interaction between carboxylic acid and thiol groups, ester bonds resulting from the interaction between primary amine groups and thiols, disulfide bonds created by the interaction of two thiol groups, and Au–S and Ag–S bonds where thiol groups interact with gold or silver. Noncovalent conjugation encompasses both electrostatic and affinity interactions.[124]

Table 2 List of the aptamers that are used to functionalize nanoparticles for targeted drug delivery to cancer cells

Aptamer	Nanomaterial	Drug	Target	Cancer cell line	Ref.
A10, RNA	PLA–PEG–COOH	Rho-labelled dextran	PSMA	Prostate cancer	99
A10, RNA	PLA–PEG–COOH	Docetaxel	PSMA	Prostate cancer	100
A10, RNA	PLA–PEG–COOH	Cisplatin	PSMA	Prostate cancer	101
A10, RNA	SPION	Doxorubicin	PSMA	LNCaP cell line	102
A10, RNA	H40–PLA–PEG	Doxorubicin	PSMA	CWR22Rγ1 cells	103
A10, RNA	PLGA	Triplex forming oligonucleotide	PSMA	LNCaP cells	104
A10-3.2, RNA	PEG–PAMAM	mRNA	PSMA	Prostate cancer	105
A10-3.2, RNA	Atelocollagen	mRNA	PSMA	Prostate cancer	106
A10, RNA and DUP-1	PEG–gold nanostar	None (PTT)	Prostate cell	Prostate cancer	107
A9, RNA	SPION	Doxorubicin	PSMA	LNCaP cell line	108
A9, RNA	ONT–PAMAM dendrimer	Doxorubicin	PSMA	Prostate cancer	109
AS1411, DNA	Liposome	Cisplatin	Nucleolin	MCF-7 cells	110
AS1411, DNA	PEG–PLGA	Paclitaxel	Nucleolin	Glioma	111
AS1411, DNA	PLGA–lecithin–PGA	Paclitaxel	Nucleolin	GI-1 and MCF-7 cells	112
AS1411, DNA	PLGA	Paclitaxel	Nucleolin	GI-1 cells	113
AS1411, DNA	PEG–PCL	Docitaxel, DiR, coumarin-6	Nucleolin	bEnd.3 and C6 cells	114
AS1411, DNA	Mesoporous silica	Gold nanorods	Nucleolin	MCF-7 cells	115
AS1411, DNA	Mesoporous silica	Fluorescein	Nucleolin	MDA-MB 231	116
AS1411, DNA	DNA nanotrains	DOX, EPI and DAU	Nucleolin	HeLa cells	117
Sgc8c, DNA	Aptamer DNA	Antisense ONT to P-gp	CCRF-CEM cells	ALL	118
S2.2, DNA	ZnO nanoparticle	Doxorubicin	Mucin-1	MCF-7 cells	119
5TR1, DNA	PLGA–chitosan	Epirubicin	Mucin-1	MCF-7 cells c26 cells	120
S15, DNA	PEG–PCL	Paclitaxel	NSCLC	A549 cells	121

The latter includes streptavidin–biotin and avidin–biotin interactions, while the former involves a linker molecule facilitating the interaction between the aptamer and nanoparticle through opposing charges. Most reported aptamer–nanoparticle conjugates are direct and covalent.[125] Farokhzad *et al.* suggested that covalently attached aptamer nanoparticles were extremely stable in physiological salts and pH.[10]

9. Aptamer–biological material conjugation for cancer therapy

Biological materials, which are biocompatible and naturally occurring, are designed to perform, enhance, or substitute natural functions, primarily for medicinal and pharmaceutical applications. Aptamers have been integrated with various biological materials, such as RNAi reagents, microsomes, antibodies, and DNA origami. These innovative conjugates are employed in the treatment of numerous diseases, including cancer, diabetes, and rheumatoid arthritis.[126]

9.1 Aptamer–antibody and short peptide conjugation

A wide range of small peptides and antibodies are produced to treat various disorders. However, these protein drugs often lack cell selectivity and efficient tumour penetration. Conjugating aptamers with short peptides and antibodies may help overcome these limitations. In 2016, Heo *et al.* developed an aptamer–antibody complex, named an oligobody, for targeted cancer therapy.[126] They conjugated an aptamer, t44-OME, to anti-cotinine antibodies. This t44-OME–anti-cotinine antibody complex penetrates cancer tissue more deeply than the antibody alone. Moreover, the anti-cotinine antibody significantly increases the pharmacokinetics of the t44-OME aptamer without affecting its affinity, indicating that the aptamer and antibody mutually enhance each other's pharmacokinetic properties. Similarly, Passariello *et al.* developed a bispecific aptamer–antibody complex.[127] This complex includes an anti-epidermal growth factor receptor (EGFR) aptamer and an anti-epidermal growth factor receptor 2 (ErbB2) compact antibody. The aptamer–antibody complex enhances the cancer cell killing ability by redirecting T cells against cancer cells. They demonstrated that this complex not only increased cell specificity but also improved the pharmacokinetics of the aptamer.

In addition to antibodies, short peptides are also combined with aptamers to enhance their specificity and bioactivity. Rajabnejad *et al.* developed an aptamer–peptide conjugate,[128] comprising an anti-nucleolin aptamer (AS1411) and the short peptide metilin, which targeted cancer cells. Metilin, a 26-amino acid peptide, is renowned for its anticancer properties. However, many studies have found that, while metilin is effective against cancer, it also causes significant adverse effects such as hemolysis and liver injury. Pusuluri *et al.* introduced a new aptamer–peptide conjugate incorporating chemotherapy drugs to enhance potency.[129] In this study, they conjugated a drug preloaded peptide (doxorubicin and camptothecin (CPT)) with an anti-nucleolin aptamer, aiming to avoid suboptimal exposure to individual drugs. Typically, chemotherapy drug combinations are administered at maximum tolerated doses, which can cause severe side effects and reduce therapeutic efficiency. However, the aptamer–peptide conjugate has the potential to mitigate these limitations. This conjugate achieved effective anti-tumor activity *in vivo* with an optimal drug concentration, approximately 500 μg kg^{-1} dose of doxorubicin and 350 μg kg^{-1} dose of CP.

9.2 Aptamer–nucleic acid drug conjugation

The emergence of RNA interference (RNAi) in 1990 paved the way for the use of nucleic acid drugs to treat a wide range of disorders.[144] Today, a variety of nucleic acid drugs, including antisense nucleotides, miRNA, siRNA, mRNA, and aptamers, have been developed. Additionally, various delivery platforms are being designed to transport these drugs.[145,146] Among them, viral vectors are the most common; however, they have limitations such as immunogenicity, biohazards, and mutagenesis.[147] On the other hand, non-viral vectors like liposomes are safer but lack specificity and efficiency.[148,149] Therefore, there is a need for a more specific and biologically secure delivery system for nucleic acid-based drugs. Consequently, the aptamer–siRNA complex has been extensively investigated over the past decade. The conjugation of aptamers and siRNA can be accomplished through covalent or non-covalent interactions. Additionally, a linker, U′–U′–U′, is often added between the aptamer and siRNA for effective delivery.[130] Since both aptamers and siRNA are nucleic acid drugs, complementary annealing is also used for their conjugation. Zhou *et al.* introduced the concept of a sticky bridge to enhance aptamer–siRNA conjugation.[131] This aptamer–siRNA complex has been shown to inhibit HIV-1 replication and infectivity in cultured T cells and primary blood mononuclear cells. Recently, Jeong *et al.* developed a multivalent aptamer–siRNA complex to overcome multiple drug resistance in various cancer cells.[132] This conjugate is constructed using an aptamer against mucin-1, siRNA against bcl-2 genes, and the chemotherapeutic drug doxorubicin.

9.3 Aptamer–DNA nanostructure conjugation

Due to its low immunogenicity and excellent biocompatibility, DNA is ideal for a variety of biological applications.[154] Furthermore, the programmable structure of DNA can significantly contribute to DNA nanotechnology, enabling the design of smart drug delivery systems. Additionally, the three-dimensional structure and form of DNA are adjustable, with its size maintainable at around 50 nm, which is optimal for cell entry. Despite its high delivery rate, DNA alone lacks targeting and precision, necessitating the integration of aptamers to enhance specificity.[133–137] Since both aptamers and DNA are derived from nucleic acid components, aptamers can be easily integrated into DNA structures. Zhu *et al.* constructed a DNA nanotrain by assembling aptamers onto DNA *via* complementary sequences.[138] Similarly, Han *et al.* developed a DNA tetrahedron by conjugating anti-cancer aptamers.[139,140]

Chemotherapy drugs such as doxorubicin often cause significant side effects, reducing the quality of therapy. Doxorubicin, with its excellent binding affinity to DNA duplexes, can be integrated into aptamer–DNA complexes to minimize adverse effects on healthy cells and tissues. Zeng *et al.* demonstrated this by creating a DOX-integrated aptamer–DNA complex, which reduced the side effects typically associated with doxorubicin.[141,142] In addition to enhancing targeted efficacy, aptamers facilitate regulated drug release in DNA–aptamer complexes. Church and colleagues initially developed an aptamer–DNA origami combination for the encapsulation and targeted delivery of thrombin to cancer blood vessels. The anti-nucleolin aptamer in this complex has molecular triggering activity, aiding in the release of the chemotherapeutic drug thrombin from the complex. This integration not only targets drug delivery but also ensures controlled release, maximizing therapeutic efficacy while minimizing side effects[143] (Fig. 4).

10. Aptamer–non-biological material conjugation for cancer therapy

Beyond biological materials, significant advancements have been made in a diverse array of nanomaterials, including micelles, hydrogels, gold nanoparticles, silica nanoparticles, and liposomes, for biomedical applications. The development of new synthesis and characterization techniques has empowered researchers to meticulously design nanomaterials with precise control over their size, shape, and properties. These nanoparticles boast unique attributes, such as a large surface area, high loading capacity, flexibility, and the enhanced permeability and retention (EPR) effect, making them outstanding candidates for therapeutic use.[154,155] Additionally, certain nanomaterials exhibit extraordinary features, like the surface plasmon resonance phenomenon. To further enhance their therapeutic potential, nanoparticles are often conjugated with targeted ligands, such as aptamers, improving their efficacy and specificity.

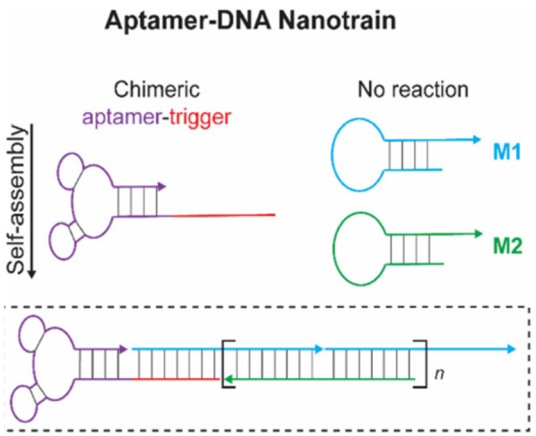

Fig. 4 Schematic representation of DNA nanostructure assembly. DNA nanotrain containing aptamers assembled by complementarity of the sequence.[138]

10.1 Aptamer–polymeric nanoparticle conjugation

These particles, ranging in size from 1 to 1000 nm, have proved to be highly effective in the targeted delivery of drugs for various disorders. Numerous polymeric nanoparticles, including micelles, hydrogels, and branched polymeric structures, are currently being developed and investigated.[154] Micelles, which are polymeric nanospheres composed of amphiphilic copolymer blocks formed through a thermodynamic process, offer numerous advantages as nanocarriers. These benefits include strong biodegradability, biocompatibility, a high drug payload capacity, and extended circulation and retention times.[155] Additionally, the hydrophobic reservoir cores of micelles aid in the delivery of poorly soluble drug. To enhance their application, researchers have begun modifying the micelle nanostructure by incorporating targeting ligands such as aptamers. The idea of aptamer–micelle conjugation was first introduced by Miyamoto and colleagues in 2007.[144] Following that, a number of aptamer–micelle conjugates were developed for medicinal purposes. In general, aptamers are conjugated to micelles using a variety of techniques, including click chemistry,[157] base-pairing hybridization,[158] and 1-ethyl-3-(3-dimethylaminopropyl)carbodiimide (EDC)-mediated conjugation.[159] In the aptamer–micelle complex, the aptamer acts as a probe for cancer-related markers such as EGFR,[160] MUC1,[161] PTK7 (protein tyrosine kinase),[138] PSMA (prostate-specific membrane antigen),[115] and HER2 (human epidermal growth factor 2).[162] Xu *et al.* created a spherical-shaped aptamer–micelle conjugate with a diameter of 69 nm by coating a unimolecular micelle on the surface of the aptamer.[103] In this case, the aptamer was chosen to target the prostate cancer biomarker PSMA. The DOX-loaded aptamer–micelle complex exhibited higher cytotoxic activity against PSMA-positive CWR22Rv1 cancer cells compared to the aptamer-free DOX–micelle complex.[163] Subsequently, a number of aptamers targeting different cell lines, including MDA-MB-231 cells[145] and Ramos cells,[146] were incorporated into micelles. In 2009, Wu *et al.* developed a micelle structure functionalized with an aptamer targeting Ramos cells.[146] The other benefits offered by aptamers to micelle nanostructures include increased cellular take up and reduced systemic toxicity. In 2015, Li *et al.* developed a micelle nanostructure consisting of AS1411 aptamers, the amphiphilic polymer Pluronic F127, and CD-PELA copolymers, employed to deliver DOX to human breast tumours.[147] The results showed that aptamer AS1411 in the micelle nanostructure improved the cellular take up and cell specificity of doxorubicin *via* nucleolin-mediated endocytosis.

For further applications, the aptamer–micelle nanostructure is conjugated to functional elements such as imaging agents and stimuli-responsive components. For example, in 2014, Tian *et al.* developed a multifunctional micelle–aptamer nanostructure by combining a NIR photosensitizer (R16FP) and a pH-active fluorescent probe (BDP-668).[145] In this conjugate, the NIR photosensitizer mediated the lysoso-

mal destruction of cancer cells by generating reactive oxygen species (ROS), while BDP-668 enhanced the visualization of therapeutic changes in real-time.

Hydrogels represent another category of polymeric nanomaterials, composed of hydrophilic and cross-linked polymeric networks. These materials are designed to respond to various stimuli, including pH,[148] temperature,[149] light exposure,[150] magnetic fields,[151] and ionic strength.[152] The conjugation of aptamers with hydrogels has a range of applications in the biomedical field, such as targeted delivery, capture and release of molecules, enhanced control of the gel–sol transition, and volume changes.[153] However, the high material permeability of hydrogels limits their application in controlled drug delivery, making it challenging to achieve precise drug release. Incorporating aptamers into hydrogels *via* an oligo-driven gel–sol transition may provide a solution to this limitation.[154] In 2008, Yang *et al.* designed a hydrogel cross-linked with an adenosine-specific aptamer system.[155] The gel–sol transition of this system, triggered by adenosine binding, was monitored by a gold nanoparticle, facilitating selective drug release. Following this, Wang *et al.* developed aptamer-conjugated hydrogel systems for the selective capture and release of individual proteins and cells.[156–159] They also created an aptamer-incorporated hydrogel capable of releasing BB-PDGF (B chain platelet-derived growth factor) by controlling analyte–ligand binding. Additionally, they designed a capture-and-release aptamer–hydrogel complex for cancer cells.[160] Future research may focus on the potential of these systems for tissue remodeling and regeneration.

10.2 Aptamer–gold nanoparticle conjugation

Gold nanoparticles are highly valued in biomedical applications due to their diverse physical and chemical properties. Advances in synthesis techniques further enhance their versatility across various applications.[161] Their optical, electrical, magnetic, and biochemical properties make them desirable for diverse uses including bioimaging, drug delivery, radiation, and photothermal therapy.[162–165] Recently, there has been increasing interest in functionalizing gold nanoparticles with aptamers. Numerous aptamer-functionalized gold nanomaterials have been developed, with a predominant focus on applications in cancer therapy. Wu *et al.* developed a nanosystem composed of Ag, Au, and aptamer S2.2, specifically targeting the MUC1 cell surface biomarker highly expressed in breast cancer MCF-7 cells.[166] This system utilizes inherent surface-enhanced Raman scattering (SERS) for bioimaging and phototherapy applications. Aptamers with structure-switching capabilities enable controlled drug release, facilitating precise and selective drug delivery. In 2012, Wang *et al.* introduced a nanocomplex comprising gold nanorods (Au NRs), an aptamer switch probe (ASP), and the photosensitizer Ce6 (Chlorine6), utilized for targeted photodynamic therapy (PDT) and photothermal therapy (PTT).[193] ASP undergoes structural changes in the presence of cancer cells, displacing Ce6 from the gold nanostructure's surface to induce singlet oxygen for PDT. The radiation absorbed by AuNRs further enhances cell death through PTT, resulting in a synergistic therapeutic effect. The inherent PTT property of gold nanoparticles offers potential for novel combination cancer therapies. Yang *et al.* then developed the Apt–AuNP–GO nanocomplex, combining aptamer-functionalized gold nanoparticles with graphene oxide, which exhibited therapeutic efficacy against cancer cells through near-infrared (NIR) light-activatable PTT.[167] This nanocomplex demonstrates a therapeutic response in cultured human breast cancer cells by modulating heat shock proteins. Building upon this approach, Yang *et al.* engineered a therapeutic complex comprising aptamers, gold nanoparticles (NPs), graphene oxide (GO), and an HSP 70 inhibitor, showcasing beneficial therapeutic effects for breast cancer cells. Recent advancements also include image-guided therapies facilitated by aptamer–gold NP complexes. For instance, He and colleagues developed aptamers selected against A549 cells, labeling Raman-tagged gold nanoparticles in 2019 for combined chemo-PTT.[168] Incorporating a Raman signal agent (4-MBA) into gold NPs, this conjugate demonstrates promising properties for targeting and eliminating cancer cells.

This evolving field underscores the potential of aptamer-functionalized gold nanoparticles for enhancing targeted therapies and advancing the frontier of cancer treatment through innovative nanoengineering approaches.

10.3 Aptamer–magnetic nanoparticle conjugation

The inherent super-paramagnetism of magnetic nanoparticles has led to their use in a variety of applications, including drug administration, MRI, cancer therapy, and individual cell isolation.[169–172] To enhance their properties for specific molecular capture and collection, these magnetic nanoparticles are often functionalized with aptamers. In 2013, Dai *et al.* introduced a novel nanosystem by incorporating an anti-multidrug-resistant-bacteria (MDRB) aptamer onto a magnetic core–plasmonic shell (MCPS).[173] In this nanocarrier, aptamer S8-7 helps to hold methylene blue (MB), which is used for fluorescence imaging and photodynamic therapy (PDT). Additionally, the gold coating on this nanocarrier enables the combined photothermal destruction of target bacteria, demonstrating its potential as a multifunctional therapeutic tool for MDRB in clinical practice. Furthermore, the photothermal therapy (PTT) efficiency of magnetic nanoparticles can be enhanced by incorporating aptamers with exceptional tumour-targeting capabilities. Aravind *et al.* developed a new aptamer-loaded magnetic fluid nanoparticle system in 2013, which included a paclitaxel-loaded fluorescent label for targeted chemotherapy, optical imaging, and drug release.[174] The aptamer in this complex targets nucleolin, a protein, the increased expression of which is linked to a poorer cancer prognosis. This system not only delivers paclitaxel *via* the nucleolin-specific aptamer (NSA) but also has the potential to magnetically direct the payload to tumour regions. In 2019, Zhao *et al.* designed a nanocomplex of aptamer-conjugated Fe_3O_4@carbon@DOX for combined chemophotothermal therapy (CPTT).[175] Aptamer sgc8 in this nanocomplex targets the lung cancer cell line A549. This nanocomplex exhibits enhanced photothermal conversion

efficiency and pH or heat-induced DOX release during PTT. Additionally, the system reduces the contrast enhancement of MRI signals, indicating its potential as a contrast agent for MRI.

10.4 Aptamer–mesoporous silica nanoparticle conjugation

MSNs (mesoporous silica nanoparticles), a ceramic material, are potential candidates for targeted drug delivery.[176,177] Advances in synthesis techniques have improved their pore size, surface area, and structure, resulting in a high drug loading capacity and facilitating the incorporation of various functional groups.[178–181] Aptamers offer numerous advantages as targeting ligands for MSNs. In therapeutic applications, Ap–MSN (aptamer–mesoporous nanoparticle) complexes are primarily intended as drug release regulators, nanocarriers, and drug trackers. Gao *et al.* developed an aptamer–MSN complex consisting of thrombin-binding aptamers, lipid-coated MSNs, and the chemotherapeutic drug docetaxel (DTX).[182,183] This aptamer@MSN@DTX complex exhibits excellent anticancer activity in thrombin-overexpressing cancer cells. Furthermore, the structure-switching properties of aptamers, when binding to target cells, enhance the drug-releasing mechanism of the aptamer–MSN complex.[184,185] In 2012, He *et al.* incorporated an ATP-responsive aptamer onto MSNs. This nanosystem includes two single-stranded DNA molecules (ssDNA1 and ssDNA2) along with the aptamer and MSNs. The nanocomplex is designed so that the aptamer is initially hybridized with two DNA sequences, and the resulting complex is conjugated to the MSN *via* the click chemistry technique. This approach blocks the pores of MSNs, preventing loss of the loaded substance. The presence of ATP enhances the interaction between the aptamer and the target, facilitating their separation from the nanoparticle complex and resulting in the release of drug molecules. In 2017, Li *et al.* used the EpCAM aptamer, an overexpressed surface biomarker in human colon adenocarcinomas, to functionalize MSN carriers for transporting the anticancer drug DM1 to colorectal cancer cells.[186] The incorporated aptamer not only facilitates drug delivery but also reduces systemic toxicity. Additionally, dopamine HCL (PDA), a pH-responsive agent, was conjugated to MSNs to regulate the release of DM1 in the EpCAM-positive SW480 colon cancer cell line in response to pH stimuli.

10.5 Aptamer–carbon nanomaterial conjugation

Currently, one-dimensional carbon nanotubes (CNTs) are attracting significant scientific interest as drug carriers and biosensors. Their unique characteristics, such as large surface area, easy modifiability, and high *in vivo* stability, make them promising for biomedical applications. Incorporating aptamers and CNTs enhances their therapeutic efficacy. The strong affinity of these targeting ligands has led to notable advancements in the aptamer–CNT field within a short period.[187–191]

This section discusses recent efforts made to develop carbon nanomaterial–aptamer conjugates that have been found to enhance therapeutic delivery. In 2015, Mohammadi *et al.* designed an RNA aptamer-incorporated single-walled carbon nanotube (SWNT) complex that significantly improved cancer therapy efficacy.[187] The nanosystem consists of EpCAM-targeting RNA aptamers, SWNTs, and a piperazine–PEA derivative (polyethyleneimine), specifically targeting EpCAM-expressing cancer cells. The aptamer@SWNT@PPEA combination effectively targets EpCAM-positive cancer cells and promotes apoptosis by inhibiting BCL91. Aptamer-incorporated SWNTs are not only effective drug carriers but also promising agents for photodynamic therapy (PDT). Following this concept, Zhu *et al.* developed a novel nanosystem consisting of a DNA aptamer, SWNTs, and a photosensitizer for controllable singlet oxygen generation (SOG).[189] In the absence of the target α-thrombin, the photosensitizer quenches SOG. However, when the target is present, the aptamer detaches from the SWNT surface and binds to the target. Additionally, a chemotherapy drug, daunorubicin, was linked to a leukemia-targeting aptamer–SWNT to enhance pH-dependent drug delivery into T-cells.[192] Recently, an aptamer-incorporated SWNT was developed for NIR laser-controlled cancer treatment. The SWNT is conjugated with an aptamer specific for sgc8, controlled by complementary DNA strands. NIR laser exposure causes the dehybridization of the DNA strands, allowing the aptamer to recognize the target and release the drug DOX.[190]

11. Biophysical approach for aptamer-based targeted drug delivery

The biophysical approach for drug delivery involves applying physics and biology principles to the design and optimisation of drug delivery systems for improved therapeutic outcomes. The objective is to comprehend the physical interactions between drug carriers, therapeutic agents, and biological systems in order to develop efficient and targeted drug delivery strategies.[193] Utilising the biophysical properties of drug carriers and their interactions with the biological environment, this strategy enhances the specificity, efficacy, and safety of drug delivery.[194]

11.1 Spectra assisted methods

The UV-Vis spectroscopic method is employed to analyse the specific interaction between an aptamer and its target. The dissociation constant (K_d) is calculated by measuring the changes in absorbance as the target concentration varies, while the aptamer concentration remains constant.[195] Generally, this method is used in drug delivery, particularly to confirm the conjugation of drugs, aptamers and nanoparticles. Zhao *et al.* developed aptamer-functionalized Fe_3O_4@carbon@doxorubicin nanoparticles for chemophotothermal therapy.[175] The UV-Vis spectrum of this aptamer-functionalized nanosystem shows a significant distinction from that of free DOX (Fig. 5 [175]). The UV-Vis spectra are measured before and after aptamer conjugation to evaluate the effectiveness of aptamer coupling with the nanocomplex. After aptamer conjugation, the peak shifts to 260 nm compared to the nanocomplex without the aptamer,

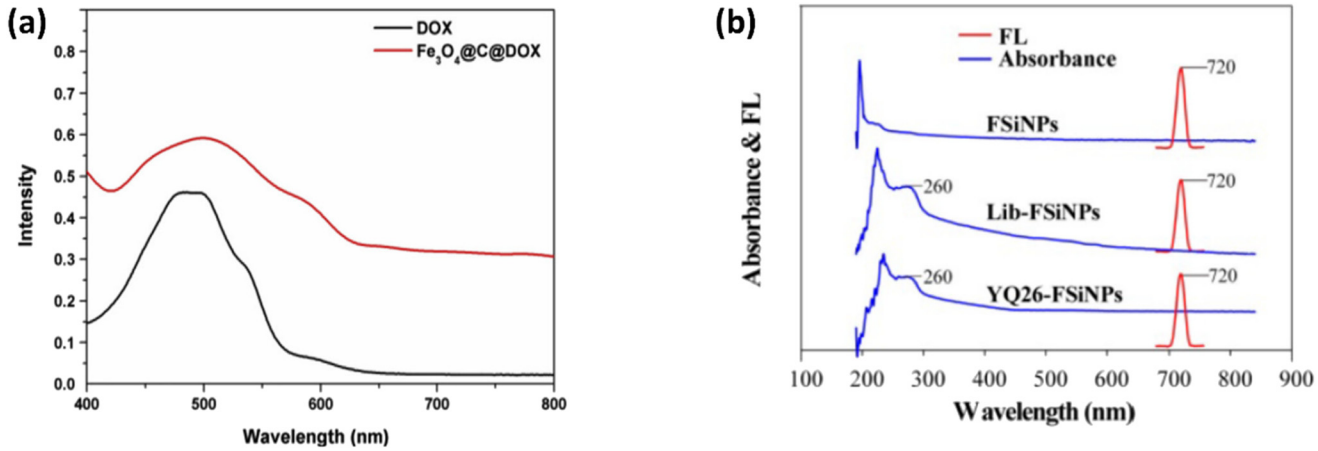

Fig. 5 UV-Vis spectras of (a) DOX and Fe_3O_4@C@DOX; the red line represents the Fe_3O_4 @C@DOX complex while the black line represents free DOX. (b) YQ26-FSiNPs, Lib-FSiNPs, and FSiNPs the blue lines represents FSiNPs, Lib-FSiNPs, and YQ26-FSiNPs, respectively. All three show an absorption peak at 260 nm.[196]

indicating successful conjugation. Tan *et al.* developed a novel theragnostic system using endoglin aptamer-conjugated fluorescent nanoparticles. The UV-Vis spectra of YQ26-FSiNPs and Lib-FSiNPs showed a DNA absorbance peak at 260 nm, which was absent in the nanoparticle complex without the aptamer (FSiNPs), further confirming the successful conjugation of the aptamer to the nanoparticle complex (illustrated in Fig. 5b [196]).

FT-IR is another spectroscopic technique used to characterize aptamer–nanoparticle conjugation by identifying the functional groups involved. Tan *et al.* performed FT-IR spectral analysis on the YQ26-FSiNPs nanocomplex to verify the presence of functional groups in the aptamer–nanocomplex.[196] The results indicated that both the complex with and without the aptamer exhibited absorption peaks at 1100 cm^{-1} and 1660 cm^{-1}, corresponding to Si–O stretching vibrations and carbonyl stretching (C═O) vibrations, respectively. Additionally, the YQ26-FSiNPs complex showed an extra peak at 1550 cm^{-1} due to amide II stretching, confirming the successful conjugation of the YQ26 aptamer to the nanocomplex.

Circular dichroism (CD) is a spectrum-assisted technique used to analyze conformational changes in aptamer structures during the formation of secondary structures.[197,198] In 2011, Lin *et al.* identified the secondary structure of an aptamer using CD spectra,[198] while Bowser *et al.* reported that different secondary structures exhibited distinct CD spectra patterns. For example, a G-quadruplex shows a negative band at 255 nm and positive bands at 245 and 290 nm.[195] Furthermore, this spectroscopic method is useful for understanding structural changes in aptamers during their binding interactions with targets.

11.2 Surface morphological studies

There are numerous techniques for investigating the morphological properties of aptamers and aptamer–NP complexes, including XPS (X-ray photoelectron spectroscopy) and TEM (transmission electron microscopy). Generally, XPS is used to determine the elemental composition of a surface.[197,199,200] Guo *et al.* developed aptamer-functionalized PEG–PLGA nanoparticles for improved anti-glioma drug delivery.[111] In their study, XPS was employed to identify the elements present in the aptamer–nanoparticle complex. The investigation revealed that the C_{1s} spectrum contained four peaks at around 285.0 eV, 286.8 eV, 287.6 eV, and 289.4 eV, with the 286.8 eV peak representing C–O–C bonds of the PEG component. Additionally, O_{1s} decomposition confirmed the existence of two forms of oxygen: O–C and O═C, at 532.7 eV and 533.6 eV, respectively. The peak at 132 eV corresponded to $P2p_3$, which was identified at 0.1% of the total number of C, O, N, and P atoms in the aptamer–nanocomplex. Based on the chemical composition, they concluded that phosphorus could only be attributed to the aptamer, confirming the incorporation of the aptamer onto the nanoparticle surface.

TEM is another technique used to study surface morphology. In the same study, Guo *et al.* also employed TEM to examine the surface morphology of the aptamer–nanoparticle complex. The study revealed that both types of nanoparticles had a spherical shape, smooth surface, and moderate uniformity. Additionally, TEM results indicated that Ap–PTX–NP had a slightly larger spherical volume compared to PTX–NP[111] (Fig. 6 [111]). In a separate study, Xu *et al.* developed aptamer-incorporated doxorubicin–unimolecular micelles for targeted therapy of prostate cancer. TEM analysis revealed that the micelles were spherical with diameters ranging from 20 to 37 nm.[103] Later, in 2019, Wen *et al.* created core–shell bifunctional nanoprobes and investigated morphological changes during the formation of the core–shell structure through TEM analysis. These observations confirmed the formation of AuNC/SiO_2/Apt nanoprobes.[201] Additionally, Tao *et al.* developed aptamer–nanoparticle conjugates for breast cancer therapy, utilizing TEM to examine the morphology of the

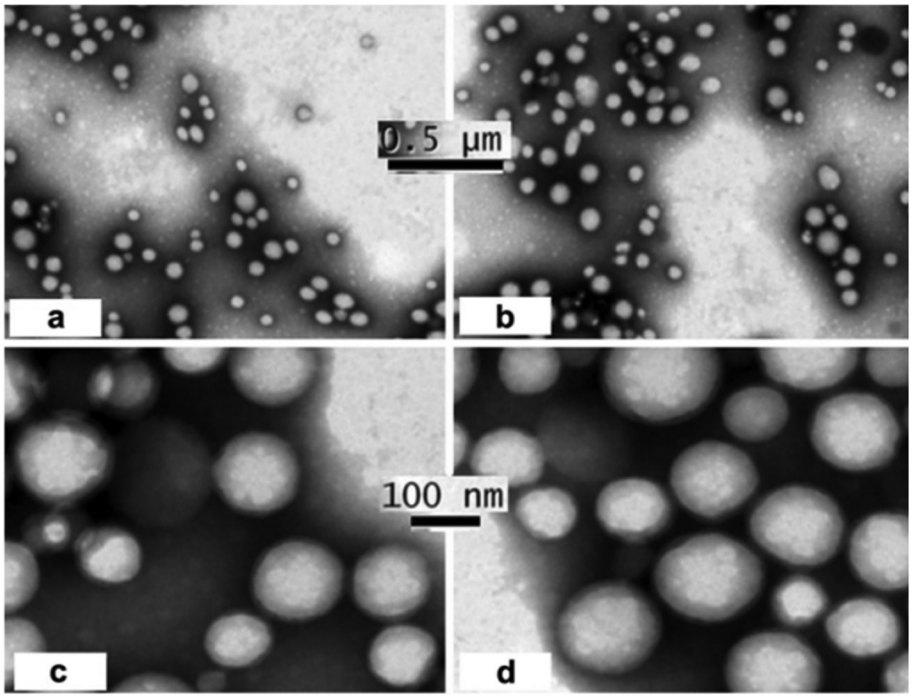

Fig. 6 TEM images of PTX-NPs (a & c) and AP-PTX NPs (b & d).[111]

aptamer–nanoparticle complex. The TEM images indicated that the complex exhibited a spherical shape with an average particle size of 90 nm.[202]

11.3 Affinity chromatography

HPLC (high performance liquid chromatography) techniques are used to analyse aptamer–target binding both qualitatively and quantitatively. This involves the pressurized passage of a liquid solvent through an aptamer-immobilized adsorbent column. The interaction is evaluated by plotting analyte concentrations against retention time on a chromatogram. This method provides insights into the equilibrium distribution of aptamer, target, and aptamer–target complexes, which can be utilized to estimate the K_d value.[203] Furthermore, HPLC can assess the binding affinity of aptamers. Deng *et al.* employed affinity chromatography techniques to study the binding interaction of a DNA aptamer to adenosine. Specifically, frontal chromatography was used to quantitatively evaluate column loading and the dissociation constant (K_d) of the immobilized aptamer.[203]

11.4 Electrophoresis

Electrophoresis, employed to analyze aptamer–target interactions, encompasses various forms such as GE (gel electrophoresis), ACE (affinity capillary electrophoresis), and ME (microchip electrophoresis). GE is a common technique for examining aptamer–target affinity interactions. Aptamers, being negatively charged, exhibit negative electrophoretic mobility, while target proteins typically show minimal polar mobility. The resulting aptamer–protein tertiary complex displays moderate electrophoretic mobility.[195] Techniques like P-labelling of nucleic acids (NAs), UV-absorbance spectra, and staining of aptamers and proteins are available for analysing aptamer concentrations in aptamer–target complexes. Despite being sensitive and cost-effective, these methods are time-consuming.

Affinity capillary electrophoresis (ACE) serves as an alternative to gel electrophoresis, focusing on the charge and size of aptamers and targets in free solution under an electric field.[60,195] ACE is categorized as competitive and noncompetitive types. Noncompetitive ACE utilizes capillary electrophoresis (CE) assisted by laser-induced fluorescence (LIF) to analyse aptamer and protein concentrations through peak analysis.[204,205] In competitive electrophoresis, two aptamers with the same target are used, one of which is labelled with a fluorescent probe (APF). The fluorescence intensity of the APF-T complex decreases due to the competitive binding of the unlabelled aptamer (AP) with APF for the binding site, generating data with two peaks that quantify binding affinity.[205] Li and colleagues applied these concepts to investigate the thrombin affinity of 15-mer and 29-mer aptamers.[206]

Microchip electrophoresis (ME) and automated microchip electrophoresis (AME) are also utilized for electrophoresis binding studies, utilizing an intercalating fluorescent dye for molecular detection. Compared to GE and ACE, microchip electrophoresis offers advantages such as avoiding gel casting, quicker sensing times, reduced sample and reagent volumes, and the ability to characterize the binding of small

molecules.[207,208] However, their applicability in basic laboratories is limited due to the complexity of developing specialized platforms for electrophoresis.

11.5 Atomic force microscopy (AFM)

AFM (atomic force microscopy) is a scanning probe microscopy method that offers high-resolution imaging of nanoscale structures. Utilizing a cantilever, AFM can examine sample surfaces with precision and measure the affinity force between the sample and the cantilever. This capability makes AFM suitable for studying aptamer–biomolecule binding affinities.[209] Notably, AFM does not require sample fixation or dehydration, allowing the examination of cells under aqueous conditions and in their natural state.[210,211] This feature makes AFM well-suited for investigating protein surfaces and the topology of living cells.

AFM data typically include a force histogram (FH) and a topology image. The affinity force of aptamer–target binding is determined by the peak location in the adhesion measurement histogram (in pN). Miyachi *et al.* indicated that higher pN values correlated with stronger affinity forces (AF) and, consequently, higher binding affinity (BA). Topology imaging provides insights into how aptamer binding modifies the surface conformation of the target. For instance, Mosafer *et al.* used AFM to explore the morphological properties of magnetic PLGA nanoparticles in their study.[212]

11.6 Thermodynamic characterization

Microscale thermophoresis (MST) and isothermal titration calorimetry (ITC) are thermodynamically related techniques used to measure the affinity between aptamers and their targets.[213–216] In ITC, the concentration of the analyte (complementary molecule) is varied while keeping the concentration of the titrant (aptamer) constant.[217] The formation of the tertiary complex is the preferred exothermic reaction, and the cell temperature is carefully controlled to eliminate other potential exothermic sources. In aptamer–target interactions, the change in energy is directly proportional to the binding stoichiometry. Pei *et al.* developed an aptamer-tethered nanostructure and conducted an ITC study to elucidate the thermodynamic binding characteristics of DOX, EPI, or DAU to AS1411. The resulting thermodynamic parameters from this study provide insights into the intermolecular interactions between aptamer AS1411 and the loaded anthracyclines.[117] MST (microscale thermophoresis) is a relatively new biophysical technique that utilizes thermal gradient generation with an infrared laser.[218,219] The thermophoretic mobility of biomolecules, influenced by factors such as charge, molecular size, solvation shell, and conformation, determines their behavior in MST. The formation of aptamer–target complexes alters these characteristics, resulting in a measurable change in mobility that quantifies their binding affinity. Due to its speed, specificity, and versatility, MST is expected to compete effectively with other biophysical technologies in the near future.

11.7 Computational techniques (*in silico*)

11.7.1 Computational methods for *in silico* aptamer modelling. The optimal SELEX process relies on the principle that when an aptamer binds to a target, it is captured and amplified through the polymerase chain reaction (PCR). This amplification significantly increases the number of aptamer candidate molecules capable of binding to the target. High-throughput (HT) sequencing technologies have facilitated the observation and comprehension of the enrichment process in SELEX.[220] In recent times, several bioinformatics-based HT sequencing technologies have been introduced to identify potential aptamer–binding interactions.[221] These methods are used to identify high affinity sequences by evaluating the frequency, enrichment, and secondary structure of aptamers. Furthermore, new aptamers are identified by utilising AI algorithms, allowing researchers to analyse the properties and sequence of high affinity aptamers from a large pool. These *in silico* techniques increase the efficiency and success rate of aptamer selection. The current method for sequence clustering uses three categories of sequence features: full-length, fixed *k*-mers (substrings with a fixed length), and sub-sequences of various lengths. FAST Aptamer is the most commonly utilised approach for full-length sequence clustering. This method enables users to count, normalise, and rank sequences, as well as categorise them according to Levenshtein distance and calculate enrichment scores between SELEX rounds. Using FAST Aptamer with a large amount of sequence data from many SELEX datasets is typically time-consuming. Recently, various user-friendly web tools, such as FAST Aptamer 2.0 and Apta Cluster, were developed for faster clustering of large databases. At present, the majority of these algorithms compute the enrichment ratio between the SELEX cycle in order to discover an aptamer family with high affinity.[222] Many studies found that, due to factors like amplification bias and nonspecific adsorption, the aptamer candidate with the highest enrichment ratio and abundance score did not necessarily have the highest affinity. Its secondary structural information is critical for finding an active candidate. In the last few years, various databases have been created to identify aptamers by searching for structural binding motifs. Apta-Motif, MP-Bind, APTANI/APTANI2 and Apta-Trace are examples of structural motif-searching techniques that have been developed in recent years. APTANI2, an upgraded version of APTANI, was constructed using Apta-Motif.[223] It has a graphical interface that offers more detailed information on the enriched aptamers. APTANI2 selects high-frequency aptamers to find relevant structural motifs. Then RNA sub opt is used to estimate probable secondary structures based on minimum free energy (MFE). Candidates are ranked based on a score that includes both motif frequency and structural stability. MP-Bind calculates a motif-level *Z*-score using four statistical tests to determine the motif enrichment status between two or more SELEX cycles. An *n*-mer window was utilised to find motifs on each aptamer. Then, MP-Bind added the *Z*-scores of all the motifs in each aptamer to get a meta-*Z*-score for the entire aptamer.

Table 3 Different AutoDock tools and their sources

Docking software	Source	Ref.
GRAMM	https://vakser.bioinformatics.ku.edu/resources/gramm/gramm1	232 and 233
Hex	https://hexserver.loria.fr/	234 and 235
ZDOCK	https://zdock.umassmed.edu	236 and 237
HADDOCK	https://haddock.chem.uu.nl/Haddock	238 and 239
NPDock	https://genesilico.pl/NPDock	240
AutoDockTools	https://mgltools.scripps.edu	241
AutoDock	https://autodock.scripps.edu/resources/references	242

Apta-TRACE also analyses sequencing data from multiple rounds of selection. The Galaxy project, Apta-SUITE, and Apt-Compare are multipurpose programmes that analyse HT-SELEX data at many stages, making aptamer identification more realistic.[222]

11.7.2 Molecular docking. The interaction between the aptamer and target can be explored using molecular docking (MD), a computational technique based on the principle of lowest binding energy. Once a high-affinity aptamer is identified, the next step involves docking it with its target, typically a protein. This simulation enables the determination of the aptamer–target binding affinity through atomistic simulations.[222] Various AutoDock tools are available, as listed in Table 3. MD employs two main categories of docking algorithms: template-based (TB) and machine learning (ML).[224] ML algorithms predict molecular interactions using sequence and structural data, while TB algorithms rely on known crystal structures of aptamers and target molecules for prediction.[225] Additionally, MD helps identify potential binding sites and elucidate the mode of interaction between aptamer and target.[226] The effectiveness of aptamer–target interactions depends on structural features such as bulges, hairpins, pseudoknots, and G-quadruplexes, enabling binding *via* electrostatic interactions, π-stacking, hydrophobic interactions, hydrogen bonding, van der Waals forces, or combinations thereof.[227] Moreover, the flexibility of an aptamer—whether rigid or flexible—affects its binding mechanism. Rigid aptamers bind like a lock and key, maintaining their structure, whereas flexible aptamers can adapt their structure to fit the target's epitope.[228]

In summary, MD simulations provide deeper insights into aptamer–target interactions, crucial for optimizing and rationally designing DNA aptamers.[229] For instance, Zhang *et al.* developed the ssDNA aptamer Z100 against zearalenone (ZEN) and employed *in silico* docking analysis using AutoDock Vina version 1.1.2 to investigate their interaction, resulting in a binding free energy of approximately −9.6 kcal mol^{-1}.[230] Similarly, Farahbakhsh *et al.* conducted an *in silico* study on aptamer AS1411 targeting nucleolin in cancer cells, identifying the SS2-55 and SS4-54 loops as active sites through molecular docking simulations.[231]

11.7.3 Molecular dynamics. The function of an aptamer is intricately tied to its molecular structure, which is influenced by factors such as local molecular environment, temperature, pH, solvated ions, and other variables. Therefore, optimizing both the structure and length of aptamers is crucial for tailoring their properties. Despite the challenges in aptamer structure modelling, atomistic computational techniques like molecular dynamics (MD) can generate realistic molecular models. For instance, Xiao *et al.* and their team utilized microsecond-scale, all-atom GPU-based MD simulations to explore how thrombin responds molecularly to aptamer binding.[243] Their study focused on comparing the mechanical properties and free energy landscapes of free thrombin *versus* thrombin bound to an aptamer. By analysing residue fluctuations and coupling, they revealed the allosteric effects induced by aptamer binding at the atomic level, particularly highlighting regions such as exosite II, 60s and sodium loops, and the alpha helix region in the light chains, which play critical roles in these allosteric modifications.[244] This level of detail helps elucidate previously observed phenomena and predicts mechanisms such as reduced autolysis rates following aptamer interaction. To conduct these simulations, they employed the GPU-enabled ACEMD simulation package, maintaining conditions of 1 atm pressure and a temperature of 300 K using Langevin damping with a damping constant of 0.10 and Berendsen pressure control with a relaxation time of 400 fs. Similarly, Xiao *et al.* employed MD simulations to compare aptamer–growth factor interactions in the presence and absence of the receptor PDGFRb. Their study characterized the aptamer–growth factor complex structure to identify binding sites across the complex, revealing reduced mobility of both molecules after complex formation between PDGF-B and its aptamer.[243]

12. Conclusion

This review delves into the specifics of aptamer-functionalized nanoparticles in cancer therapy, highlighting their potential as a targeted treatment option. Aptamers, short single-stranded oligonucleotides, possess unique properties that make them highly suitable for targeted therapy. Given the off-target effects associated with conventional chemotherapy and other treatment modalities, there is an urgent need for innovative therapeutic strategies in cancer treatment. This landscape is conducive to the advancement of targeted drug delivery systems. Aptamer-functionalized nanoparticles emerge as promising candidates for anticancer therapy. Traditional nano-mediated drug delivery primarily relies on the enhanced permeability

and retention (EPR) effect, which has inherent limitations. In contrast, receptor-mediated targeting using aptamer-functionalized nanoparticles can circumvent these drawbacks. Despite growing interest in these active targeting ligands, their clinical application remains limited. Therefore, addressing the current state of aptamers is crucial for optimizing their efficacy and minimizing side effects.

This review traces the journey from the discovery of the first aptamer in 1990 to the latest advancements in SELEX, various *in silico* approaches, and the development of diverse aptamer-functionalized nanoparticles. By revisiting the literature and examining current innovations, we aim to chart a course for future research into the potential of these active targeting ligands in cancer treatment. Adopting a biophysical approach, we explore a range of quantitative and qualitative methods to analyse molecular interactions, physical properties, and behaviours of aptamer–nanoparticle conjugates. This understanding is vital for the effective development of these conjugates for applications in medicine, diagnostics, and beyond. By gaining deeper insights into these interactions, we can better harness the potential of aptamer-functionalized nanoparticles in targeted cancer therapy.

13. Challenges and future perspective

Aptamer-incorporated nanoparticles hold immense promise for advancing anticancer drug development and applications. Despite growing interest in these active targeting ligands, their clinical and preclinical use remains limited. To fully leverage the potential of aptamers while minimizing side effects, it is essential to address their current state.

In 1996, the United States FDA approved the first nanotechnology-based anticancer drug, which encapsulated doxorubicin in PEGylated liposomes. Today, approximately ten nanoparticle-based cancer drugs have received approval from the FDA or other agencies and are commercially available. These drugs are either untargeted or passively targeted, extending the drug's half-life and reducing side effects to some extent. However, the therapeutic improvements have been marginal, and off-target effects remain a significant issue, highlighting the need for actively targeted nanoparticles. Currently, over a dozen nanoparticles for cancer therapy are in clinical trials, with many featuring active targeting. However, none of these employ aptamer functionalization. Actively targeted nanoparticles, particularly those functionalized with aptamers, possess tremendous potential for future nanodrug development and applications. Therefore, intensified research efforts, improved experimental designs, and overcoming barriers to clinical translation are imperative. A major obstacle to the clinical application of aptamer-conjugated nanoparticles is limited information on their target effects and toxicity in animals or humans. Additionally, the availability of aptamers for clinical use is restricted. Aptamers, as short single-stranded nucleic acids, are prone to degradation in nuclease-rich physiological environments. Most aptamers reported in the scientific literature are obtained through *in vitro* selection, raising concerns about their *in vivo* affinity under physiological conditions. Thus, innovative aptamer stabilization techniques and SELEX (systematic evolution of ligands by exponential enrichment) strategies are urgently needed. Before clinical trials can commence, the biosafety of aptamer-based nanomedicines must be thoroughly evaluated. Aptamers contain foreign nucleic acids, posing risks of genomic insertion and immune responses. Additionally, some aptamer-functionalized materials exhibit inherent cytotoxicity. For example, cadmium-containing quantum dots (QDs) have been shown to induce DNA damage in cells and exhibit high toxicity. Systematic toxicity evaluations of candidate aptamer-integrated remedies are essential to ensure biosafety in clinical trials.

In summary, this innovative approach to aptamer–nanoparticle conjugation offers profound insights that are crucial for developing a highly effective and specific aptamer-functionalized nanoparticle system for cancer therapy. Addressing the current limitations and challenges is imperative to fully harness the potential of these advanced systems. By overcoming these hurdles, the door to the successful clinical application of aptamer-functionalized nanoparticles in targeted cancer therapy can be opened, promising a new era in cancer treatment.

Author contributions

Alanthatta Govindan Navaneeth: first author, literature survey, main script writing. Subramani Karthikeyan: corresponding author, main script correction.

Data availability

No primary research results, software or code have been included and no new data were generated or analysed as part of this review.

Conflicts of interest

The authors report there are no competing interests to declare.

Acknowledgements

The authors thank VIT University for providing a VIT RGMES SEED GRANT for carrying out this research work.

References

1 J. Ferlay, M. Colombet, I. Soerjomataram, *et al.*, Cancer statistics for the year 2020: An overview, *Int. J. Cancer*, 2021, **149**, 778–789.
2 P. A. Jones and S. B. Baylin, The epigenomics of cancer, *Cell*, 2007, **128**, 683–692.

3 T. N. Seyfried and L. C. Huysentruyt, On the origin of cancer metastasis, *Crit. Rev. Oncog.*, 2013, **18**, 43–73.
4 I. J. Fidler, Cancer metastasis, *Br. Med. Bull.*, 1991, **47**, 157–177.
5 N. Behranvand, F. Nasri, R. Zolfaghari Emameh, *et al.*, Chemotherapy: a double-edged sword in cancer treatment, *Cancer Immunol. Immunother.*, 2022, **71**, 507–526, DOI: **10.1007/s00262-021-03013-3**.
6 R. Liu, C. Luo, Z. Pang, *et al.*, Advances of nanoparticles as drug delivery systems for disease diagnosis and treatment, *Chin. Chem. Lett.*, 2023, **34**, 107518.
7 M. A. Subhan, F. Parveen, N. Filipczak, *et al.*, Approaches to Improve EPR-Based Drug Delivery for Cancer Therapy and Diagnosis, *J. Pers. Med.*, 2023, **13**, 389.
8 J. A. Stephenson, J. C. Goddard, O. Al-Taan, *et al.*, Tumour Angiogenesis: A Growth Area—From John Hunter to Judah Folkman and Beyond, *J. Cancer Res.*, 2013, **2013**, 1–6.
9 S. Gavas, S. Quazi and T. M. Karpiński, Nanoparticles for Cancer Therapy: Current Progress and Challenges, *Nanoscale Res. Lett.*, 2021, **16**(1), 173.
10 O. C. Farokhzad, J. M. Karp and R. Langer, Nanoparticle-aptamer bioconjugates for cancer targeting, *Expert Opin. Drug Delivery*, 2006, **3**, 311–324.
11 Z. Fu and J. Xiang, Aptamer-functionalized nanoparticles in targeted delivery and cancer therapy, *Int. J. Mol. Sci.*, 2020, **21**, 1–39.
12 C. Tuerk and L. Gold, Systematic evolution of ligands by exponential enrichment: RNA ligands to bacteriophage T4 DNA polymerase, *Science*, 1990, 505–510.
13 R. Stoltenburg, C. Reinemann and B. Strehlitz, SELEX – A (r)evolutionary method to generate high-affinity nucleic acid ligands, *Biomol. Eng.*, 2007, **24**, 381–403.
14 J. Zhou and J. Rossi, Aptamers as targeted therapeutics: Current potential and challenges, *Nat. Rev. Drug Discovery*, 2017, **16**, 181–202.
15 D. Proske, M. Blank, R. Buhmann, *et al.*, Aptamers – Basic research, drug development, and clinical applications, *Appl. Microbiol. Biotechnol.*, 2005, **69**, 367–374.
16 R. D. Jenison, S. C. Gill, A. Pardi, *et al.*, High-resolution molecular discrimination by RNA, *Science*, 1994, **263**, 1425–1429.
17 M. M. Soldevilla, H. Villanueva and F. Pastor, Aptamers: a feasible technology in cancer immunotherapy, *J. Immunol. Res.*, 2016, **2016**, 1083738.
18 K. Ghasemii, M. Darroudi, I. Rahimmanesh, *et al.*, Advances in aptamer-based drug delivery vehicles for cancer therapy, *Biomater. Adv.*, 2022, **140**, 213077.
19 A. Wochner, M. Menger and M. Rimmele, Characterisation of aptamers for therapeutic studies, *Expert Opin. Drug Discovery*, 2007, **2**, 1205–1224.
20 C. Chandola and M. Neerathilingam, Aptamers for targeted delivery: current challenges and future opportunities, *Role Nov. Drug Deliv. Veh. Nanobiomedicine*, 2019, pp. 1–22.
21 A. V. Lakhin, V. Z. Tarantul and L. V. Gening, Aptamers: problems, solutions and prospects, *Acta Nat.*, 2013, **5**, 34–43.
22 J. B.-H. Tok, J. Cho and R. R. Rando, RNA aptamers that specifically bind to a 16S ribosomal RNA decoding region construct, *Nucleic Acids Res.*, 2000, **28**, 2902–2910.
23 L. C. Bock, L. C. Griffin, J. A. Latham, *et al.*, Selection of single-stranded DNA molecules that bind and inhibit human thrombin, *Nature*, 1992, **355**, 564–566, DOI: **10.1038/355564a0**.
24 M. F. Kubik, A. W. Stephens, D. Schneider, *et al.*, High-affinity RNA ligands to human alpha-thrombin, *Nucleic Acids Res.*, 1994, **22**, 2619–2626.
25 R. White, C. Rusconi, E. Scardino, *et al.*, Generation of species cross-reactive aptamers using "toggle" SELEX, *Mol. Ther.*, 2001, **4**, 567–573.
26 T. M. A. Gronewold, S. Glass, E. Quandt, *et al.*, Monitoring complex formation in the blood-coagulation cascade using aptamer-coated SAW sensors, *Biosens. Bioelectron.*, 2005, **20**, 2044–2052.
27 P. Colas, B. Cohen, T. Jessen, *et al.*, Genetic selection of peptide aptamers that recognize and inhibit cyclin-dependent kinase 2, *Nature*, 1996, **380**, 548–550.
28 R. Yazdian-Robati, M. Ramezani, M. Khedri, *et al.*, An aptamer for recognizing the transmembrane protein PDL-1 (programmed death-ligand 1), and its application to fluorometric single cell detection of human ovarian carcinoma cells, *Microchim. Acta*, 2017, **184**, 4029–4035. Available from: **https://api.semanticscholar.org/CorpusID:102924897**.
29 P. Colas, The eleven-year switch of peptide aptamers, *J. Biol.*, 2008, **7**, 2.
30 I. C. Baines and P. Colas, Peptide aptamers as guides for small-molecule drug discovery, *Drug Discovery Today*, 2006, **11**, 334–341.
31 F. Hoppe-Seyler, I. Crnkovic-Mertens, C. Denk, *et al.*, Peptide aptamers: new tools to study protein interactions, *J. Steroid Biochem. Mol. Biol.*, 2001, **78**, 105–111.
32 S. J. Choi and C. Ban, Crystal structure of a DNA aptamer bound to PvLDH elucidates novel single-stranded DNA structural elements for folding and recognition, *Sci. Rep.*, 2016, **6**, 1–13.
33 D. O'Connell, A. Koenig, S. Jennings, *et al.*, Calcium-dependent oligonucleotide antagonists specific for L-selectin, *Proc. Natl. Acad. Sci. U. S. A.*, 1996, **93**, 5883–5887.
34 K. E. Maier and M. Levy, From selection hits to clinical leads: progress in aptamer discovery, *Mol. Ther. – Methods Clin. Dev.*, 2016, **3**, 16014, DOI: **10.1038/mtm.2016.14**.
35 S. Ni, Z. Zhuo, Y. Pan, *et al.*, Recent Progress in Aptamer Discoveries and Modifications for Therapeutic Applications, *ACS Appl. Mater. Interfaces*, 2021, **13**, 9500–9519.
36 K. Li, J. Deng, H. Jin, *et al.*, Chemical modification improves the stability of the DNA aptamer GBI-10 and its affinity towards tenascin-C, *Org. Biomol. Chem.*, 2017, **15**, 1174–1182, DOI: **10.1039/C6OB02577C**.
37 A. L. Chang, M. McKeague and C. D. Smolke, Facile characterization of aptamer kinetic and equilibrium

binding properties using surface plasmon resonance, *Methods Enzymol*, Elsevier, 2014, pp. 451–466.

38 A. Abe, S. Kosugi, K. Yoshida, *et al.*, Genome sequencing reveals agronomically important loci in rice using MutMap, *Nat. Biotechnol.*, 2012, **30**, 174–178, DOI: 10.1038/nbt.2095.

39 B. Santosh and P. K. Yadava, Nucleic acid aptamers: research tools in disease diagnostics and therapeutics, *BioMed Res. Int.*, 2014, **2014**, 540451.

40 Z. Zhuo, Y. Yu, M. Wang, *et al.*, Recent advances in SELEX technology and aptamer applications in biomedicine, *Int. J. Mol. Sci.*, 2017, **18**, 1–19.

41 Y. Lei, X. He, J. Tang, *et al.*, Ultra-pH-responsive split i-motif based aptamer anchoring strategy for specific activatable imaging of acidic tumor microenvironment, *Chem. Commun.*, 2018, **54**, 10288–10291.

42 S. Kolesnikova and E. A. Curtis, Structure and Function of Multimeric G-Quadruplexes, *Molecules*, 2019, **24**, 3074.

43 A. A. Novoseltseva, N. M. Ivanov, R. A. Novikov, *et al.*, Structural and Functional Aspects of G-Quadruplex Aptamers Which Bind a Broad Range of Influenza A Viruses, *Biomolecules*, 2020, **10**(1), 119.

44 T. Sakamoto, E. Ennifar and Y. Nakamura, Thermodynamic study of aptamers binding to their target proteins, *Biochimie*, 2018, **145**, 91–97. Available from: https://www.sciencedirect.com/science/article/pii/S0300908417302626.

45 J. R. Williamson, Induced fit in RNA–protein recognition, *Nat. Struct. Biol.*, 2000, **7**, 834–837, DOI: 10.1038/79575.

46 S. Jones, D. T. Daley, N. M. Luscombe, *et al.*, Protein-RNA interactions: a structural analysis, *Nucleic Acids Res.*, 2001, **29**, 943–954.

47 M. Rimmele, Nucleic acid aptamers as tools and drugs: recent developments, *ChemBioChem*, 2003, **4**, 963–971.

48 Y. Feng, T. T. Baig, R. P. Love, *et al.*, Suppression of APOBEC3-mediated restriction of HIV-1 by Vif, *Front. Microbiol.*, 2014, **5**, 450.

49 R. D. Jenison, S. C. Gill, A. Pardi, *et al.*, High-resolution molecular discrimination by RNA, *Science*, 1994, **263**(5152), 1425–1429.

50 M. Michaud, E. Jourdan, A. Villet, *et al.*, A DNA aptamer as a new target-specific chiral selector for HPLC, *J. Am. Chem. Soc.*, 2003, **125**, 8672–8679.

51 P. R. Bouchard, R. M. Hutabarat and K. M. Thompson, Discovery and development of therapeutic aptamers, *Annu. Rev. Pharmacol. Toxicol.*, 2010, **50**, 237–257.

52 T. Wang, C. Chen, L. M. Larcher, *et al.*, Three decades of nucleic acid aptamer technologies: Lessons learned, progress and opportunities on aptamer development, *Biotechnol. Adv.*, 2019, **37**, 28–50. Available from: https://www.sciencedirect.com/science/article/pii/S0734975018301770.

53 D. Musumeci and D. Montesarchio, Polyvalent nucleic acid aptamers and modulation of their activity: a focus on the thrombin binding aptamer, *Pharmacol. Ther.*, 2012, **136**, 202–215.

54 C. Platella, C. Riccardi, D. Montesarchio, *et al.*, G-quadruplex-based aptamers against protein targets in therapy and diagnostics, *Biochim. Biophys. Acta, Gen. Subj.*, 2017, **1861**, 1429–1447.

55 L. Li, Q. Yin, J. Cheng, *et al.*, Polyvalent mesoporous silica nanoparticle-aptamer bioconjugates target breast cancer cells, *Adv. Healthc. Mater.*, 2012, **1**, 567–572.

56 P. C. Patel, D. A. Giljohann, D. S. Seferos, *et al.*, Peptide antisense nanoparticles, *Proc. Natl. Acad. Sci. U. S. A.*, 2008, **105**, 17222–17226.

57 X. Lin, Q. Chen, W. Liu, *et al.*, Assay of multiplex proteins from cell metabolism based on tunable aptamer and microchip electrophoresis, *Biosens. Bioelectron.*, 2015, **63**, 105–111.

58 C. M. Barbieri, T.-K. Li, S. Guo, *et al.*, Aminoglycoside Complexation with a DNA·RNA Hybrid Duplex: The Thermodynamics of Recognition and Inhibition of RNA Processing Enzymes, *J. Am. Chem. Soc.*, 2003, **125**, 6469–6477.

59 R. Wang, J. Zhao, T. Jiang, *et al.*, Selection and characterization of DNA aptamers for use in detection of avian influenza virus H5N1, *J. Virol. Methods*, 2013, **189**, 362–369.

60 M. McKeague, E. M. McConnell, J. Cruz-Toledo, *et al.*, Analysis of in vitro aptamer selection parameters, *J. Mol. Evol.*, 2015, **81**, 150–161.

61 F. Almasi, S. L. Mousavi Gargari, F. Bitaraf, *et al.*, Development of a Single Stranded DNA Aptamer as a Molecular Probe for LNCap Cells Using Cell-SELEX, *Avicenna J. Med. Biotechnol.*, 2016, **8**, 104–111.

62 K. Setlem, B. Mondal, S. Ramlal, *et al.*, Immuno Affinity SELEX for Simple, Rapid, and Cost-Effective Aptamer Enrichment and Identification against Aflatoxin B1, *Front. Microbiol.*, 2016, **7**, 1909.

63 L. Wang, R. Wang, F. Chen, *et al.*, QCM-based aptamer selection and detection of Salmonella typhimurium, *Food Chem.*, 2017, **221**, 776–782.

64 S. D. Mendonsa and M. T. Bowser, In Vitro Selection of Aptamers with Affinity for Neuropeptide Y Using Capillary Electrophoresis, *J. Am. Chem. Soc.*, 2005, **127**, 9382–9383, DOI: 10.1021/ja052406n.

65 S. D. Mendonsa and M. T. Bowser, In Vitro Evolution of Functional DNA Using Capillary Electrophoresis, *J. Am. Chem. Soc.*, 2004, **126**, 20–21, DOI: 10.1021/ja037832s.

66 L. Dong, Q. Tan, W. Ye, *et al.*, Screening and Identifying a Novel ssDNA Aptamer against Alpha-fetoprotein Using CE-SELEX, *Sci. Rep.*, 2015, **5**, 15552, DOI: 10.1038/srep15552.

67 N. S. Hamedani and J. Müller, Capillary Electrophoresis for the Selection of DNA Aptamers Recognizing Activated Protein C, *Methods Mol. Biol.*, 2016, **1380**, 61–75.

68 S. D. Mendonsa and M. T. Bowser, In vitro selection of high-affinity DNA ligands for human IgE using capillary electrophoresis, *Anal. Chem.*, 2004, **76**, 5387–5392.

69 R. K. Mosing and M. T. Bowser, Isolating Aptamers Using Capillary Electrophoresis–SELEX (CE–SELEX), in *Nucleic Acid and Peptide Aptamers, Methods and Protocols*, ed. G. Mayer, Humana Press, Totowa, NJ, 2009, pp. 33–43. DOI: 10.1007/978-1-59745-557-2_3.

70 S. R. Watson, Y. F. Chang, D. O'Connell, *et al.*, Anti-L-selectin aptamers: binding characteristics, pharmacokinetic parameters, and activity against an intravascular target in vivo, *Antisense Nucleic Acid Drug Dev.*, 2000, **10**, 63–75.
71 J. Wang, T. Gao, Y. Luo, *et al.*, In vitro selection of a DNA aptamer by cell-SELEX as a molecular probe for cervical cancer recognition and imaging, *J. Mol. Evol.*, 2019, **87**, 72–82.
72 Y. Zheng, Y. Zhao, Y. Di, *et al.*, DNA aptamers from whole-serum SELEX as new diagnostic agents against gastric cancer, *RSC Adv.*, 2019, **9**, 950–957.
73 Y. Zhao, L. He, B. Huang, *et al.*, Identification of a novel DNA aptamer that selectively targets lung cancer serum, *RSC Adv.*, 2021, **11**, 33759–33769.
74 Y. Guo, K. Li, Y. Gao, *et al.*, CLEC3B Identified as a Potential Lung Cancer Biomarker in Serum by Aptamer-Capture Technology, *ChemistrySelect*, 2021, **6**, 5640–5645.
75 B. J. Hicke, C. Marion, Y. F. Chang, *et al.*, Tenascin-C aptamers are generated using tumor cells and purified protein, *J. Biol. Chem.*, 2001, **276**, 48644–48654.
76 K. Germer, M. Leonard and X. Zhang, RNA aptamers and their therapeutic and diagnostic applications, *Int. J. Biochem. Mol. Biol.*, 2013, **4**, 27.
77 B. J. Hicke, A. W. Stephens, T. Gould, *et al.*, Tumor targeting by an aptamer, *J. Nucl. Med.*, 2006, **47**, 668–678.
78 A. C. Girvan, Y. Teng, L. K. Casson, *et al.*, AGRO100 inhibits activation of nuclear factor-kappaB (NF-kappaB) by forming a complex with NF-kappaB essential modulator (NEMO) and nucleolin, *Mol. Cancer Ther.*, 2006, **5**, 1790–1799.
79 C. S. M. Ferreira, C. S. Matthews and S. Missailidis, DNA aptamers that bind to MUC1 tumour marker: design and characterization of MUC1-binding single-stranded DNA aptamers, *Tumour Biol.*, 2006, **27**, 289–301.
80 M. I. A. de Melo, C. R. Correa, P. da Silva Cunha, *et al.*, DNA aptamers selection for carcinoembryonic antigen (CEA), *Bioorg. Med. Chem. Lett.*, 2020, **30**, 127278.
81 K. Li, L. Qi, L. Gao, *et al.*, Selection and preliminary application of a single stranded DNA aptamer targeting colorectal cancer serum, *RSC Adv.*, 2019, **9**, 38867–38876.
82 D. Ferreira, J. Barbosa, D. A. Sousa, *et al.*, Selection of aptamers against triple negative breast cancer cells using high throughput sequencing, *Sci. Rep.*, 2021, **11**, 8614, DOI: **10.1038/s41598-021-87998-y**.
83 S. E. Lupold, Aptamers and apple pies: a mini-review of PSMA aptamers and lessons from Donald S. Coffey, *Am. J. Clin. Exp. Urol.*, 2018, **6**, 78.
84 J. C. Leach, A. Wang, K. Ye, *et al.*, A RNA-DNA hybrid aptamer for nanoparticle-based prostate tumor targeted drug delivery, *Int. J. Mol. Sci.*, 2016, **17**, 380.
85 J. P. Dassie, X. Liu, G. S. Thomas, *et al.*, Systemic administration of optimized aptamer-siRNA chimeras promotes regression of PSMA-expressing tumors, *Nat. Biotechnol.*, 2009, **27**, 839–846.
86 W. M. Rockey, F. J. Hernandez, S.-Y. Huang, *et al.*, Rational truncation of an RNA aptamer to prostate-specific membrane antigen using computational structural modeling, *Nucleic Acid Ther.*, 2011, **21**, 299–314.
87 J. J. Trausch, M. Shank-Retzlaff and T. Verch, Development and characterization of an HPV Type-16 specific modified DNA aptamer for the improvement of potency assays, *Anal. Chem.*, 2017, **89**, 3554–3561.
88 C. Li, S. Yang, R. Li, *et al.*, Dual-Aptamer-Targeted Immunomagnetic Nanoparticles to Accurately Explore the Correlations between Circulating Tumor Cells and Gastric Cancer, *ACS Appl. Mater. Interfaces*, 2022, **14**, 7646–7658, DOI: **10.1021/acsami.1c22720**.
89 E. Kim, M. Kang and C. Ban, Aptamer-antibody hybrid ELONA that uses hybridization chain reaction to detect a urinary biomarker EN2 for bladder and prostate cancer, *Sci. Rep.*, 2022, **12**, 1–14.
90 X. Sun, L. Xie, S. Qiu, *et al.*, Elucidation of CKAP4-remodeled cell mechanics in driving metastasis of bladder cancer through aptamer-based target discovery, *Proc. Natl. Acad. Sci. U. S. A.*, 2022, **119**, e2110500119.
91 B. Suwussa, C. Tao, S. Mohammed Ibrahim, *et al.*, Pattern Recognition of Cancer Cells Using Aptamer-Conjugated Magnetic Nanoparticles, *ACS Nano*, 2012, **6**(5), 3974–3981.
92 S. Li, H. Xu, H. Ding, *et al.*, Identification of an aptamer targeting hnRNP A1 by tissue slide-based SELEX, *J. Pathol.*, 2009, **218**, 327–336.
93 W. Zhong, Y. Pu, W. Tan, *et al.*, Identification and Application of an Aptamer Targeting Papillary Thyroid Carcinoma Using Tissue-SELEX, *Anal. Chem.*, 2019, **91**, 8289–8297.
94 P. Bayat, R. Nosrati, M. Alibolandi, *et al.*, SELEX methods on the road to protein targeting with nucleic acid aptamers, *Biochimie*, 2018, **154**, 132–155, DOI: **10.1016/j.biochi.2018.09.001**.
95 L. Zhou, P. Li, M. Yang, *et al.*, Generation and characterization of novel DNA aptamers against coat protein of grouper nervous necrosis virus (GNNV) with antiviral activities and delivery potential in grouper cells, *Antiviral Res.*, 2016, **129**, 104–114.
96 A. Ozer, B. S. White, J. T. Lis, *et al.*, Density-dependent cooperative non-specific binding in solid-phase SELEX affinity selection, *Nucleic Acids Res.*, 2013, **41**, 7167–7175.
97 J. G. Bruno and J. L. Kiel, Use of magnetic beads in selection and detection of biotoxin aptamers by electrochemiluminescence and enzymatic methods, *BioTechniques*, 2002, **32**, 178–180, 182–183.
98 E. Dausse, A. Barré, A. Aimé, *et al.*, Aptamer selection by direct microfluidic recovery and surface plasmon resonance evaluation, *Biosens. Bioelectron.*, 2016, **80**, 418–425.
99 P. Magala, W. E. Bocik, A. Majumdar, *et al.*, Conformational Dynamics Modulate Activation of the Ubiquitin Conjugating Enzyme Ube2g2, *ACS Omega*, 2017, **2**, 4581–4592.

100 D Shangguan, Y Li, Z Tang, *et al.*, Aptamers Evolved from Live Cells as Effective Molecular Probes for Cancer Study, *Proc. Natl. Acad. Sci. U. S. A.*, 2006, **103**(32), 11838–11843, DOI: https://doi.org/10.1073/pnas.0602615103..

101 S. Dhar, F. X. Gu, R. Langer, *et al.*, Targeted delivery of cisplatin to prostate cancer cells by aptamer functionalized Pt(IV) prodrug-PLGA-PEG nanoparticles, *Proc. Natl. Acad. Sci. U. S. A.*, 2008, **105**, 17356–17361.

102 A. Z. Wang, V. Bagalkot, C. C. Vasilliou, *et al.*, Superparamagnetic iron oxide nanoparticle-aptamer bioconjugates for combined prostate cancer imaging and therapy, *ChemMedChem*, 2008, **3**, 1311–1315.

103 W. Xu, I. A. Siddiqui, M. Nihal, *et al.*, Aptamer-conjugated and doxorubicin-loaded unimolecular micelles for targeted therapy of prostate cancer, *Biomaterials*, 2013, **34**, 5244–5253.

104 Y. H. Lee and G. G. Song, Un co r re c te d Un co r re c te d, *Neoplasma*, 2013, **60**, 607–616.

105 X. Wu, Z. Tai, Q. Zhu, *et al.*, Study on the prostate cancer-targeting mechanism of aptamer-modified nanoparticles and their potential anticancer effect in vivo, *Int. J. Nanomed.*, 2014, **9**, 5431–5440.

106 Z. Hao, W. Fan, J. Hao, *et al.*, Efficient delivery of micro RNA to bone-metastatic prostate tumors by using aptamer-conjugated atelocollagen in vitro and in vivo, *Drug Delivery*, 2016, **23**, 874–881.

107 H. Jo, H. Youn, S. Lee, *et al.*, Ultra-effective photothermal therapy for prostate cancer cells using dual aptamer-modified gold nanostars, *J. Mater. Chem. B*, 2014, **2**, 4862–4867, DOI: 10.1039/C4TB00643G.

108 I.-H. Lee, S. An, M. K. Yu, *et al.*, Targeted chemoimmunotherapy using drug-loaded aptamer-dendrimer bioconjugates, *J. Controlled Release*, 2011, **155**, 435–441.

109 M. K. Yu, D. Kim, I.-H. Lee, *et al.*, Image-guided prostate cancer therapy using aptamer-functionalized thermally cross-linked superparamagnetic iron oxide nanoparticles, *Small*, 2011, **7**, 2241–2249.

110 Z. Cao, R. Tong, A. Mishra, *et al.*, Reversible cell-specific drug delivery with aptamer-functionalized liposomes, *Angew. Chem., Int. Ed.*, 2009, **48**, 6494–6498.

111 J. Guo, X. Gao, L. Su, *et al.*, Aptamer-functionalized PEG-PLGA nanoparticles for enhanced anti-glioma drug delivery, *Biomaterials*, 2011, **32**, 8010–8020, DOI: 10.1016/j.biomaterials.2011.07.004.

112 A. Aravind, P. Jeyamohan, R. Nair, *et al.*, AS1411 aptamer tagged PLGA-lecithin-PEG nanoparticles for tumor cell targeting and drug delivery, *Biotechnol. Bioeng.*, 2012, **109**, 2920–2931.

113 A. Aravind, S. H. Varghese, S. Veeranarayanan, *et al.*, Aptamer-labeled PLGA nanoparticles for targeting cancer cells, *Cancer Nanotechnol.*, 2012, **3**, 1–12.

114 H. Gao, J. Qian, S. Cao, *et al.*, Precise glioma targeting of and penetration by aptamer and peptide dual-functioned nanoparticles, *Biomaterials*, 2012, **33**, 5115–5123.

115 X. Yang, X. Liu, Z. Liu, *et al.*, Near-infrared light-triggered, targeted drug delivery to cancer cells by aptamer gated nanovehicles, *Adv. Mater.*, 2012, **24**, 2890–2895.

116 F. J. Hernandez, L. I. Hernandez, A. Pinto, *et al.*, Targeting cancer cells with controlled release nanocapsules based on a single aptamer, *Chem. Commun.*, 2013, **49**, 1285–1287.

117 W. Pei, M. Liu, Y. Wu, *et al.*, High payload and targeted release of anthracyclines by aptamer-tethered DNA nanotrains – Thermodynamic and release kinetic study, *Eur. J. Pharm. Sci.*, 2020, **148**, 105319, DOI: 10.1016/j.ejps.2020.105319.

118 C. Wu, D. Han, T. Chen, *et al.*, Building a multifunctional aptamer-based DNA nanoassembly for targeted cancer therapy, *J. Am. Chem. Soc.*, 2013, **135**, 18644–18650.

119 Z. Han, X. Wang, C. Heng, *et al.*, Synergistically enhanced photocatalytic and chemotherapeutic effects of aptamer-functionalized ZnO nanoparticles towards cancer cells, *Phys. Chem. Chem. Phys.*, 2015, **17**, 21576–21582, DOI: 10.1039/C5CP02139A.

120 S. Taghavi, M. Ramezani, M. Alibolandi, *et al.*, Chitosan-modified PLGA nanoparticles tagged with 5TR1 aptamer for in vivo tumor-targeted drug delivery, *Cancer Lett.*, 2017, **400**, 1–8.

121 D. Barak, S. Engelberg, Y. G. Assaraf, *et al.*, Selective Targeting and Eradication of Various Human Non-Small Cell Lung Cancer Cell Lines Using Self-Assembled Aptamer-Decorated Nanoparticles, *Pharmaceutics*, 2022, **14**, 1650.

122 O. C. Farokhzad, A. Khademhosseini, S. Jon, *et al.*, Microfluidic system for studying the interaction of nanoparticles and microparticles with cells, *Anal. Chem.*, 2005, **77**, 5453–5459.

123 D. Sehgal and I. K. Vijay, A method for the high efficiency of water-soluble carbodiimide-mediated amidation, *Anal. Biochem.*, 1994, **218**, 87–91.

124 O. C. Farokhzad, S. Jon, A. Khademhosseini, *et al.*, Nanoparticle-aptamer bioconjugates: a new approach for targeting prostate cancer cells, *Cancer Res.*, 2004, **64**, 7668–7672.

125 P. Ray and R. R. White, Aptamers for targeted drug delivery, *Pharmaceuticals*, 2010, **3**, 1761–1778.

126 K. Heo, S.-W. Min, H. J. Sung, *et al.*, An aptamer-antibody complex (oligobody) as a novel delivery platform for targeted cancer therapies, *J. Controlled Release*, 2016, **229**, 1–9.

127 M. Passariello, S. Camorani, C. Vetrei, *et al.*, Novel Human Bispecific Aptamer-Antibody Conjugates for Efficient Cancer Cell Killing, *Cancers*, 2019, **11**, 1268.

128 S. H. Rajabnejad, A. Mokhtarzadeh, K. Abnous, *et al.*, Targeted delivery of melittin to cancer cells by AS1411 anti-nucleolin aptamer, *Drug Dev. Ind. Pharm.*, 2018, **44**, 982–987.

129 A. Pusuluri, V. Krishnan, V. Lensch, *et al.*, Treating Tumors at Low Drug Doses Using an Aptamer-Peptide Synergistic Drug Conjugate, *Angew. Chem., Int. Ed.*, 2019, **58**, 1437–1441.

130 A. Gilboa-Geffen, P. Hamar, M. T. N. Le, *et al.*, Gene Knockdown by EpCAM Aptamer-siRNA Chimeras

Suppresses Epithelial Breast Cancers and Their Tumor-Initiating Cells, *Mol. Cancer Ther.*, 2015, **14**, 2279–2291.

131 J. Zhou, P. Swiderski, H. Li, *et al.*, Selection, characterization and application of new RNA HIV gp 120 aptamers for facile delivery of Dicer substrate siRNAs into HIV infected cells, *Nucleic Acids Res.*, 2009, **37**, 3094–3109.

132 H. Jeong, S. H. Lee, Y. Hwang, *et al.*, Multivalent Aptamer-RNA Conjugates for Simple and Efficient Delivery of Doxorubicin/siRNA into Multidrug-Resistant Cells, *Macromol. Biosci.*, 2017, **17**(4), DOI: 10.1002/mabi.201600343.

133 R. M. Zadegan, M. D. E. Jepsen, L. L. Hildebrandt, *et al.*, Construction of a fuzzy and Boolean logic gates based on DNA, *Small*, 2015, **11**, 1811–1817.

134 E. S. Andersen, M. Dong, M. M. Nielsen, *et al.*, Self-assembly of a nanoscale DNA box with a controllable lid, *Nature*, 2009, **459**, 73–76.

135 V. S. Chambers, G. Marsico, J. M. Boutell, *et al.*, High-throughput sequencing of DNA G-quadruplex structures in the human genome, *Nat. Biotechnol.*, 2015, **33**, 877–881.

136 R. Hänsel-Hertsch, D. Beraldi, S. V. Lensing, *et al.*, G-quadruplex structures mark human regulatory chromatin, *Nat. Genet.*, 2016, **48**, 1267–1272.

137 A. Malugin and H. Ghandehari, Cellular uptake and toxicity of gold nanoparticles in prostate cancer cells: a comparative study of rods and spheres, *J. Appl. Toxicol.*, 2010, **30**, 212–217.

138 G. Zhu, J. Zheng, E. Song, *et al.*, Self-assembled, aptamer-tethered DNA nanotrains for targeted transport of molecular drugs in cancer theranostics, *Proc. Natl. Acad. Sci. U. S. A.*, 2013, **110**, 7998–8003.

139 Q. Li, D. Zhao, X. Shao, *et al.*, Aptamer-Modified Tetrahedral DNA Nanostructure for Tumor-Targeted Drug Delivery, *ACS Appl. Mater. Interfaces*, 2017, **9**, 36695–36701.

140 X. Han, Y. Jiang, S. Li, *et al.*, Multivalent aptamer-modified tetrahedral DNA nanocage demonstrates high selectivity and safety for anti-tumor therapy, *Nanoscale*, 2018, **11**, 339–347.

141 Y. Zeng, J. Liu, S. Yang, *et al.*, Time-lapse live cell imaging to monitor doxorubicin release from DNA origami nanostructures, *J. Mater. Chem. B*, 2018, **6**, 1605–1612.

142 C. Wiraja, Y. Zhu, D. C. S. Lio, *et al.*, Framework nucleic acids as programmable carrier for transdermal drug delivery, *Nat. Commun.*, 2019, **10**, 1147.

143 R. Jahanban-Esfahlan, K. Seidi, A. Jahanban-Esfahlan, *et al.*, Static DNA Nanostructures For Cancer Theranostics: Recent Progress In Design And Applications, *Nanotechnol., Sci. Appl.*, 2019, **12**, 25–46.

144 D. Miyamoto, Z. Tang, T. Takarada, *et al.*, Turbidimetric detection of ATP using polymeric micelles and DNA aptamers, *Chem. Commun.*, 2007, 4743–4745.

145 J. Tian, L. Ding, H. Ju, *et al.*, A multifunctional nanomicelle for real-time targeted imaging and precise near-infrared cancer therapy, *Angew. Chem., Int. Ed.*, 2014, **53**, 9544–9549.

146 Y. Wu, K. Sefah, H. Liu, *et al.*, DNA aptamer-micelle as an efficient detection/delivery vehicle toward cancer cells, *Proc. Natl. Acad. Sci. U. S. A.*, 2010, **107**, 5–10.

147 X. Li, Y. Yu, Q. Ji, *et al.*, Targeted delivery of anticancer drugs by aptamer AS1411 mediated Pluronic F127/cyclodextrin-linked polymer composite micelles, *Nanomedicine*, 2015, **11**, 175–184.

148 B. Jeong, S. W. Kim and Y. H. Bae, Thermosensitive sol-gel reversible hydrogels, *Adv. Drug Delivery Rev.*, 2002, **54**, 37–51.

149 A. Richter, G. Paschew, S. Klatt, *et al.*, Review on Hydrogel-based pH Sensors and Microsensors, *Sensors*, 2008, **8**, 561–581.

150 Y.-L. Zhao and J. F. Stoddart, Azobenzene-based light-responsive hydrogel system, *Langmuir*, 2009, **25**, 8442–8446.

151 T.-Y. Liu, S.-H. Hu, T.-Y. Liu, *et al.*, Magnetic-sensitive behavior of intelligent ferrogels for controlled release of drug, *Langmuir*, 2006, **22**, 5974–5978.

152 R. Rodríguez, C. Alvarez-Lorenzo and A. Concheiro, Cationic cellulose hydrogels: kinetics of the cross-linking process and characterization as pH-/ion-sensitive drug delivery systems, *J. Controlled Release*, 2003, **86**, 253–265.

153 N. Zhao, A. Suzuki, X. Zhang, *et al.*, Dual Aptamer-Functionalized in Situ Injectable Fibrin Hydrogel for Promotion of Angiogenesis via Codelivery of Vascular Endothelial Growth Factor and Platelet-Derived Growth Factor-BB, *ACS Appl. Mater. Interfaces*, 2019, **11**, 18123–18132.

154 M. Liu, L. Wang, Y. Lo, *et al.*, Aptamer-Enabled Nanomaterials for Therapeutics, Targeting and Imaging, *Cells*, 2022, **11**, 159.

155 H. Yang, H. Liu, H. Kang, *et al.*, Engineering target-responsive hydrogels based on aptamer-target interactions, *J. Am. Chem. Soc.*, 2008, **130**, 6320–6321.

156 B. Soontornworajit, J. Zhou, M. P. Snipes, *et al.*, Affinity hydrogels for controlled protein release using nucleic acid aptamers and complementary oligonucleotides, *Biomaterials*, 2011, **32**, 6839–6849.

157 M. R. Battig, B. Soontornworajit and Y. Wang, Programmable release of multiple protein drugs from aptamer-functionalized hydrogels via nucleic acid hybridization, *J. Am. Chem. Soc.*, 2012, **134**, 12410–12413.

158 Z. Zhang, N. Chen, S. Li, *et al.*, Programmable hydrogels for controlled cell catch and release using hybridized aptamers and complementary sequences, *J. Am. Chem. Soc.*, 2012, **134**, 15716–15719.

159 Z. Zhang, S. Li, N. Chen, *et al.*, Programmable display of DNA-protein chimeras for controlling cell-hydrogel interactions via reversible intermolecular hybridization, *Biomacromolecules*, 2013, **14**, 1174–1180.

160 N. Zhao, M. R. Battig, M. Xu, *et al.*, Development of a Dual-Functional Hydrogel Using RGD and Anti-VEGF Aptamer, *Macromol. Biosci.*, 2017, **17**, 1700201.

161 J. Turkevich, P. C. Stevenson and J. Hillier, A study of the nucleation and growth processes in the synthesis of col-

loidal gold, *Discuss. Faraday Soc.*, 1951, **11**, 55–75, DOI: 10.1039/DF9511100055.
162 L. Cole, R. Ross, J. Tilley, *et al.*, Gold nanoparticles as contrast agents in X-ray imaging and computed tomography, *Nanomedicine*, 2015, **10**, 321–341.
163 P. Ghosh, G. Han, M. De, *et al.*, Gold nanoparticles in delivery applications, *Adv. Drug Delivery Rev.*, 2008, **60**, 1307–1315.
164 A. Nicolás-Boluda, J. Vaquero, G. Laurent, *et al.*, Photothermal Depletion of Cancer-Associated Fibroblasts Normalizes Tumor Stiffness in Desmoplastic Cholangiocarcinoma, *ACS Nano*, 2020, **14**, 5738–5753.
165 X.-D. Zhang, D. Wu, X. Shen, *et al.*, Size-dependent radiosensitization of PEG-coated gold nanoparticles for cancer radiation therapy, *Biomaterials*, 2012, **33**, 6408–6419.
166 P. Wu, Y. Gao, H. Zhang, *et al.*, Aptamer-guided silver-gold bimetallic nanostructures with highly active surface-enhanced Raman scattering for specific detection and near-infrared photothermal therapy of human breast cancer cells, *Anal. Chem.*, 2012, **84**, 7692–7699.
167 L. Yang, Y.-T. Tseng, G. Suo, *et al.*, Photothermal therapeutic response of cancer cells to aptamer-gold nanoparticle-hybridized graphene oxide under NIR illumination, *ACS Appl. Mater. Interfaces*, 2015, **7**, 5097–5106.
168 J. He, J. Dong, Y. Hu, *et al.*, Design of Raman tag-bridged core–shell Au@$Cu_3(BTC)_2$ nanoparticles for Raman imaging and synergistic chemo-photothermal therapy, *Nanoscale*, 2019, **11**, 6089–6100, DOI: 10.1039/C9NR00041K.
169 E. Taboada, E. Rodríguez, A. Roig, *et al.*, Relaxometric and magnetic characterization of ultrasmall iron oxide nanoparticles with high magnetization. Evaluation as potential T1 magnetic resonance imaging contrast agents for molecular imaging, *Langmuir*, 2007, **23**, 4583–4588.
170 D.-L. Zhao, X.-X. Wang, X.-W. Zeng, *et al.*, Preparation and inductive heating property of Fe_3O_4–chitosan composite nanoparticles in an AC magnetic field for localized hyperthermia, *J. Alloys Compd.*, 2009, **477**, 739–743.
171 T. Vangijzegem, D. Stanicki and S. Laurent, Magnetic iron oxide nanoparticles for drug delivery: applications and characteristics, *Expert Opin. Drug Delivery*, 2019, **16**, 69–78.
172 J. Gao, H. Gu and B. Xu, Multifunctional magnetic nanoparticles: design, synthesis, and biomedical applications, *Acc. Chem. Res.*, 2009, **42**, 1097–1107.
173 X. Dai, Z. Fan, Y. Lu, *et al.*, Multifunctional nanoplatforms for targeted multidrug-resistant-bacteria theranostic applications, *ACS Appl. Mater. Interfaces*, 2013, **5**, 11348–11354.
174 A. Aravind, R. Nair, S. Raveendran, *et al.*, Aptamer conjugated paclitaxel and magnetic fluid loaded fluorescently tagged PLGA nanoparticles for targeted cancer therapy, *J. Magn. Magn. Mater.*, 2013, **344**, 116–123. Available from: https://www.sciencedirect.com/science/article/pii/S030488531300365X.
175 C. Zhao, X. Song, W. Jin, *et al.*, Image-guided cancer therapy using aptamer-functionalized cross-linked magnetic-responsive Fe_3O_4@carbon nanoparticles, *Anal. Chim. Acta*, 2019, **1056**, 108–116.
176 T. Yanagisawa, T. Shimizu, K. Kuroda, *et al.*, The Preparation of Alkyltrimethylammonium–Kanemite Complexes and Their Conversion to Microporous Materials, *Bull. Chem. Soc. Jpn.*, 1990, **63**, 988–992, DOI: 10.1246/bcsj.63.988.
177 C. T. Kresge, M. E. Leonowicz, W. J. Roth, *et al.*, Ordered mesoporous molecular sieves synthesized by a liquid-crystal template mechanism, *Nature*, 1992, **359**, 710–712, DOI: 10.1038/359710a0.
178 M. Xu, Y. Wen, Y. Liu, *et al.*, Hollow mesoporous ruthenium nanoparticles conjugated bispecific antibody for targeted anti-colorectal cancer response of combination therapy, *Nanoscale*, 2019, **11**, 9661–9678, DOI: 10.1039/C9NR01904A.
179 Y.-P. Chen, C.-T. Chen, Y. Hung, *et al.*, A new strategy for intracellular delivery of enzyme using mesoporous silica nanoparticles: superoxide dismutase, *J. Am. Chem. Soc.*, 2013, **135**, 1516–1523.
180 Y. Hoshikawa, H. Yabe, A. Nomura, *et al.*, Mesoporous Silica Nanoparticles with Remarkable Stability and Dispersibility for Antireflective Coatings, *Chem. Mater.*, 2009, **22**(1), 12–14.
181 L. L. Hench, The story of Bioglass, *J. Mater. Sci. Mater. Med.*, 2006, **17**, 967–978.
182 L. Gao, Y. Cui, Q. He, *et al.*, Selective recognition of co-assembled thrombin aptamer and docetaxel on mesoporous silica nanoparticles against tumor cell proliferation, *Chem. – Eur. J.*, 2011, **17**, 13170–13174.
183 M. Alibolandi, F. Hoseini, M. Mohammadi, *et al.*, Curcumin-entrapped MUC-1 aptamer targeted dendrimer-gold hybrid nanostructure as a theranostic system for colon adenocarcinoma, *Int. J. Pharm.*, 2018, **549**, 67–75.
184 F.-F. Zheng, P.-H. Zhang, Y. Xi, *et al.*, Aptamer/Graphene Quantum Dots Nanocomposite Capped Fluorescent Mesoporous Silica Nanoparticles for Intracellular Drug Delivery and Real-Time Monitoring of Drug Release, *Anal. Chem.*, 2015, **87**, 11739–11745.
185 X. He, Y. Zhao, D. He, *et al.*, ATP-responsive controlled release system using aptamer-functionalized mesoporous silica nanoparticles, *Langmuir*, 2012, **28**, 12909–12915.
186 Y. Li, Y. Duo, S. Bao, *et al.*, EpCAM aptamer-functionalized polydopamine-coated mesoporous silica nanoparticles loaded with DM1 for targeted therapy in colorectal cancer, *Int. J. Nanomed.*, 2017, **12**, 6239–6257.
187 M. Mohammadi, Z. Salmasi, M. Hashemi, *et al.*, Single-walled carbon nanotubes functionalized with aptamer and piperazine-polyethylenimine derivative for targeted siRNA delivery into breast cancer cells, *Int. J. Pharm.*, 2015, **485**, 50–60.
188 S. Liu, L. Wei, L. Hao, *et al.*, Sharper and faster "nano darts" kill more bacteria: a study of antibacterial activity of individually dispersed pristine single-walled carbon nanotube, *ACS Nano*, 2009, **3**, 3891–3902.
189 Z. Zhu, Z. Tang, J. A. Phillips, *et al.*, Regulation of singlet oxygen generation using single-walled carbon nanotubes, *J. Am. Chem. Soc.*, 2008, **130**, 10856–10857.

190 Y. Yang, J. Liu, X. Sun, *et al.*, Near-infrared light-activated cancer cell targeting and drug delivery with aptamer-modified nanostructures, *Nano Res.*, 2016, **9**, 139–148, DOI: 10.1007/s12274-015-0898-4.
191 M. Pourmadadi, A. Moammeri, A. Shamsabadipour, *et al.*, Application of Various Optical and Electrochemical Nanobiosensors for Detecting Cancer Antigen 125 (CA-125): A Review, *Biosensors*, 2023, **13**(1), 99.
192 S. M. Taghdisi, P. Lavaee, M. Ramezani, *et al.*, Reversible targeting and controlled release delivery of daunorubicin to cancer cells by aptamer-wrapped carbon nanotubes, *Eur. J. Pharm. Biopharm.*, 2011, **77**, 200–206.
193 J. Wang, G. Zhu, M. You, *et al.*, Assembly of Aptamer Switch Probes and Photosensitizer on Gold Nanorods for Targeted Photothermal and Photodynamic Cancer Therapy, *ACS Nano.*, 2012, **6**(6), 5070–5077.
194 C. Peetla, A. Stine and V. Labhasetwar, Biophysical interactions with model lipid membranes: Applications in drug discovery and drug delivery, *Mol. Pharm.*, 2009, **6**, 1264–1276.
195 M. Jing and M. T. Bowser, Methods for measuring aptamer-protein equilibria: a review, *Anal. Chim. Acta*, 2011, **686**, 9–18.
196 J. Tan, N. Yang, L. Zhong, *et al.*, A New Theranostic System Based on Endoglin Aptamer Conjugated Fluorescent Silica Nanoparticles, *Theranostics*, 2017, **7**, 4862–4876.
197 M. McKeague and M. C. Derosa, Challenges and opportunities for small molecule aptamer development, *J. Nucleic Acids*, 2012, **2012**, 748913.
198 P.-H. Lin, R.-H. Chen, C.-H. Lee, *et al.*, Studies of the binding mechanism between aptamers and thrombin by circular dichroism, surface plasmon resonance and isothermal titration calorimetry, *Colloids Surf., B*, 2011, **88**, 552–558.
199 R. F. Macaya, P. Schultze, F. W. Smith, *et al.*, Thrombin-binding DNA aptamer forms a unimolecular quadruplex structure in solution, *Proc. Natl. Acad. Sci. U. S. A.*, 1993, **90**, 3745–3749.
200 V. J. B. Ruigrok, M. Levisson, J. Hekelaar, *et al.*, Characterization of aptamer-protein complexes by X-ray crystallography and alternative approaches, *Int. J. Mol. Sci.*, 2012, **13**, 10537–10552.
201 S. Wen, X. Miao, *et al.*, Aptamer-Conjugated Au Nanocage/SiO_2 Core-Shell Bifunctional Nanoprobes with High Stability and Biocompatibility for Cellular SERS Imaging and Near-Infrared Photothermal Therapy, *ACS Sens.*, 2019, **4**(2), 301–308, DOI: 10.1021/acssensors.8b00682.
202 W. Tao, X. Zeng, J. Wu, *et al.*, Polydopamine-based surface modification of novel nanoparticle-aptamer bioconjugates for in vivo breast cancer targeting and enhanced therapeutic effects, *Theranostics*, 2016, **6**, 470–484.
203 Q. Deng, I. German, D. Buchanan, *et al.*, Retention and separation of adenosine and analogues by affinity chromatography with an aptamer stationary phase, *Anal. Chem.*, 2001, **73**, 5415–5421.
204 D. N. Stratis-Cullum, S. McMasters and P. M. Pellegrino, Evaluation of relative aptamer binding to Campylobacter jejuni bacteria using affinity probe capillary electrophoresis, *Anal. Lett.*, 2009, **42**, 2389–2402.
205 X. C. Le, Q.-H. Wan and M. T. Lam, Fluorescence polarization detection for affinity capillary electrophoresis, *Electrophoresis*, 2002, **23**, 903–908.
206 Y. Li, L. Guo, F. Zhang, *et al.*, High-sensitive determination of human α-thrombin by its 29-mer aptamer in affinity probe capillary electrophoresis, *Electrophoresis*, 2008, **29**, 2570–2577.
207 J. Hu and C. J. Easley, A simple and rapid approach for measurement of dissociation constants of DNA aptamers against proteins and small molecules via automated microchip electrophoresis, *Analyst*, 2011, **136**, 3461–3468.
208 F. Nishikawa, H. Arakawa and S. Nishikawa, Application of microchip electrophoresis in the analysis of RNA aptamer-protein interactions, *Nucleosides, Nucleotides Nucleic Acids*, 2006, **25**, 369–382.
209 Y. Miyachi, N. Shimizu, C. Ogino, *et al.*, Selection of DNA aptamers using atomic force microscopy, *Nucleic Acids Res.*, 2010, **38**, e21.
210 L. Kailas, E. C. Ratcliffe, E. J. Hayhurst, *et al.*, Immobilizing live bacteria for AFM imaging of cellular processes, *Ultramicroscopy*, 2009, **109**, 775–780.
211 N. E. Lonergan, L. D. Britt and C. J. Sullivan, Immobilizing live Escherichia coli for AFM studies of surface dynamics, *Ultramicroscopy*, 2014, **137**, 30–39.
212 J. Mosafer, K. Abnous, M. Tafaghodi, *et al.*, In vitro and in vivo evaluation of anti-nucleolin-targeted magnetic PLGA nanoparticles loaded with doxorubicin as a theranostic agent for enhanced targeted cancer imaging and therapy, *Eur. J. Pharm. Biopharm.*, 2017, **113**, 60–74, DOI: 10.1016/j.ejpb.2016.12.009.
213 M. Kwon, S. M. Chun, S. Jeong, *et al.*, In vitro selection of RNA against kanamycin B, *Mol. Cells*, 2001, **11**, 303–311.
214 M. N. Win, J. S. Klein and C. D. Smolke, Codeine-binding RNA aptamers and rapid determination of their binding constants using a direct coupling surface plasmon resonance assay, *Nucleic Acids Res.*, 2006, **34**, 5670–5682.
215 R. Stoltenburg, C. Reinemann and B. Strehlitz, FluMag-SELEX as an advantageous method for DNA aptamer selection, *Anal. Bioanal. Chem.*, 2005, **383**, 83–91.
216 R. Stoltenburg, C. Reinemann and B. Strehlitz, SELEX – A (r)evolutionary method to generate high-affinity nucleic acid ligands, *Biomol. Eng.*, 2007, **24**, 381–403.
217 R. Stoltenburg, T. Schubert and B. Strehlitz, In vitro Selection and Interaction Studies of a DNA Aptamer Targeting Protein A, *PLoS One*, 2015, **10**, e0134403.
218 P. Amero, C. L. Esposito, A. Rienzo, *et al.*, Identification of an Interfering Ligand Aptamer for EphB2/3 Receptors, *Nucleic Acid Ther.*, 2016, **26**, 102–110.
219 C. Entzian and T. Schubert, Studying small molecule-aptamer interactions using MicroScale Thermophoresis (MST), *Methods*, 2016, **97**, 27–34.

220 M. Asmari, M. Waqas, A. E. Ibrahim, *et al.*, Microscale Thermophoresis and Molecular Modelling to Explore the Chelating Drug Transportation in the Milk to Infant, *Molecules*, 2022, **27**(14), 4604.

221 D. Sun, M. Sun, J. Zhang, *et al.*, Computational tools for aptamer identification and optimization, *TrAC, Trends Anal. Chem.*, 2022, **157**, 116767.

222 M. Sherman and L. Contreras, Computational approaches in design of nucleic acid-based therapeutics, *Curr. Opin. Biotechnol*, 2018, **53**, 232–239. Available from: **https://www.sciencedirect.com/science/article/pii/S095816691730188X**.

223 J. Caroli, C. Taccioli, A. De La Fuente, *et al.*, APTANI: A computational tool to select aptamers through sequence-structure motif analysis of HT-SELEX data, *Bioinformatics*, 2016, **32**, 161–164.

224 T. N. Navien, R. Thevendran, H. Y. Hamdani, *et al.*, In silico molecular docking in DNA aptamer development, *Biochimie*, 2021, **180**, 54–67, DOI: **10.1016/j.biochi.2020.10.005**.

225 J. Si, J. Cui, J. Cheng, *et al.*, Computational Prediction of RNA-Binding Proteins and Binding Sites, *Int. J. Mol. Sci.*, 2015, **16**, 26303–26317.

226 B. Deng, Y. Lin, C. Wang, *et al.*, Aptamer binding assays for proteins: the thrombin example – a review, *Anal. Chim. Acta*, 2014, **837**, 1–15.

227 S. Y. Tan, C. Acquah, A. Sidhu, *et al.*, SELEX Modifications and Bioanalytical Techniques for Aptamer–Target Binding Characterization, *Crit. Rev. Anal. Chem.*, 2016, **46**, 521–537.

228 T. Hayashi, H. Oshima, T. Mashima, *et al.*, Binding of an RNA aptamer and a partial peptide of a prion protein: crucial importance of water entropy in molecular recognition, *Nucleic Acids Res.*, 2014, **42**, 6861–6875.

229 V. Tereshko, E. Skripkin and D. J. Patel, Encapsulating streptomycin within a small 40-mer RNA, *Chem. Biol.*, 2003, **10**, 175–187.

230 Y. Zhang, T. Lu, Y. Wang, *et al.*, Selection of a DNA Aptamer against Zearalenone and Docking Analysis for Highly Sensitive Rapid Visual Detection with Label-Free Aptasensor, *J. Agric. Food Chem.*, 2018, **66**, 12102–12110.

231 Z. Farahbakhsh, M. R. Zamani, M. Rafienia, *et al.*, In silico activity of AS1411 aptamer against nucleolin of cancer cells, *Iran J. Blood Cancer*, 2020, **12**, 95–100.

232 E. Katchalski-Katzir, I. Shariv, M. Eisenstein, *et al.*, Molecular surface recognition: determination of geometric fit between proteins and their ligands by correlation techniques, *Proc. Natl. Acad. Sci. U. S. A.*, 1992, **89**, 2195–2199.

233 A. Tovchigrechko and I. A. Vakser, GRAMM-X public web server for protein-protein docking, *Nucleic Acids Res.*, 2006, **34**, W310–W314.

234 D. W. Ritchie and G. J. Kemp, Protein docking using spherical polar Fourier correlations, *Proteins*, 2000, **39**, 178–194.

235 D. W. Ritchie and V. Venkatraman, Ultra-fast FFT protein docking on graphics processors, *Bioinformatics*, 2010, **26**, 2398–2405.

236 B. G. Pierce, K. Wiehe, H. Hwang, *et al.*, ZDOCK server: interactive docking prediction of protein-protein complexes and symmetric multimers, *Bioinformatics*, 2014, **30**, 1771–1773.

237 Q.-L. Wang, H.-F. Cui, J.-F. Du, *et al.*, In silico post-SELEX screening and experimental characterizations for acquisition of high affinity DNA aptamers against carcinoembryonic antigen, *RSC Adv.*, 2019, **9**, 6328–6334.

238 S. J. de Vries, M. van Dijk and A. M. J. J. Bonvin, The HADDOCK web server for data-driven biomolecular docking, *Nat. Protoc.*, 2010, **5**, 883–897.

239 M. van Dijk, A. D. J. van Dijk, V. Hsu, *et al.*, Information-driven protein-DNA docking using HADDOCK: it is a matter of flexibility, *Nucleic Acids Res.*, 2006, **34**, 3317–3325.

240 I. Tuszynska, M. Magnus, K. Jonak, *et al.*, NPDock: a web server for protein-nucleic acid docking, *Nucleic Acids Res.*, 2015, **43**, W425–W430.

241 S. Forli, R. Huey, M. E. Pique, *et al.*, Computational protein-ligand docking and virtual drug screening with the AutoDock suite, *Nat. Protoc.*, 2016, **11**, 905–919.

242 V. Y. Tanchuk, V. O. Tanin, A. I. Vovk, *et al.*, A New, Improved Hybrid Scoring Function for Molecular Docking and Scoring Based on AutoDock and AutoDock Vina, *Chem. Biol. Drug Des.*, 2016, **87**, 618–625.

243 J. Xiao and F. R. Salsbury, Molecular dynamics simulations of aptamer-binding reveal generalized allostery in thrombin, *J. Biomol. Struct. Dyn.*, 2017, **35**, 3354–3369, DOI: **10.1080/07391102.2016.1254682**.

244 C. Q. Vu, P. Rotkrua, B. Soontornworajit, *et al.*, Effect of PDGF-B aptamer on PDGFRβ/PDGF-B interaction: Molecular dynamics study, *J. Mol. Graphics Modell.*, 2018, **82**, 145–156.